Exploring the visual system of the Black Grouse (*Lyrurus tetrix*): Combining experimental and molecular approaches to inform strategies for reducing collisions

Simon Potier[1*], Jean-Marc Lassance[2], Constance Blary[3], Justine Coulombier[4], Sandrine Berthillot[4], Virginie M. Dos Santos[5], Christine Andraud[6] and Marjorie A. Liénard[7*]

1 Simon Potier Expert Scientifique, Foucrainville, France

2 Laboratory of Evolutionary Neuroethology, GIGA Institute, University of Liège, 4000 Liège,

Belgium

3 CEFE, Univ Montpellier, CNRS, EPHE, IRD, Montpellier, France

4 Parc national de la Vanoise, Chambéry, France

5 Association Observatoire des Galliformes de Montagne, Sevrier, France

6 Centre de Recherche sur la Conservation des Collections, CNRS, Muséum National d'Histoire Naturelle, France

7 Laboratory of Molecular Biology of Sensory Systems, GIGA Institute, University of Liège, 4000 Liège, Belgium

Corresponding authors
*sim.potier@gmail.com; marjorie.lienard@uliege.be

ORCID IDs:

S.P.: 0000-0003-3156-7846
J-M.L.: 0000-0002-3675-6956
C.B.: 0000-0001-6204-9983
V.D.S: 0009-0008-1660-7639
VMDS: 0009-0008-1660-7639
C.A.: 0000-0002-3112-9363
M.A.L.: 0000-0003-3193-3666

Keywords: visual field, contrast vision, spectral sensitivity, opsin, bird collision

Abstract

Understanding the visual systems of birds can inform conservation efforts and mitigate the impact of anthropogenic threats. This study investigates the visual abilities of the black grouse *Lyrurus tetrix* (Galliformes: Phasianidae), a European mountain bird highly vulnerable to collisions with man-made structures. Using an integrative approach, we assessed key visual components including visual field configuration, spatial resolution, contrast sensitivity, and spectral sensitivity. Behavioral assays revealed that black grouse have an extensive visual field with a wide binocular overlap and minimal blind spots, allowing for efficient predator detection and foraging. However, their spatial resolution and contrast sensitivity are relatively low, consistent with other prey species. Molecular analyses identified four cone opsins (SWS1, SWS2, Rh2, and LW) with spectral sensitivities spanning ultraviolet to long wavelengths (393–546 nm). These findings highlight the black grouse's ability to detect UV light, which could be exploited in the context of collision mitigation. Our results emphasize the need for measures tailored to species-specific visual abilities, including diverters designed with enhanced reflectance and increased visibility. This study advances our understanding of avian vision and provides critical insights to guide conservation strategies for reducing bird collisions in alpine habitats.

Introduction

Vision is a primary sensory modality for avian species, enabling most birds to gather accurate and instantaneous environmental information from different directions and over varying distances, and to perform tasks such as foraging or predator detection (Land & Nilsson, 2012, Martin, 2017). While eyes are metabolically expensive organs and therefore usually physically constrained (Witter & Cuthill, 1993, Laughlin et al., 1998, Niven & Laughlin, 2008, Moran et al., 2015), most birds investigated to date typically have larger eyes relative to body mass (Brooke et al., 1999, Caves et al., 2024), as well as relatively more complex retinae (Crescitelli et al., 1977, Goldsmith, 1990) than other terrestrial vertebrates, supporting overall a complex visual system . Avian photoreceptors absorb photons in the retina, which then, to form images, sample visual information projected by the lens and cornea (Land & Nilsson, 2012).

Differences in visual abilities result from differences in eye morphology that meet species-specific ecological requirements shaping sophisticated detection, recognition and discrimination of objects to guide remarkable and vital behaviours such as navigation, foraging and communication. To efficiently perform these tasks, birds need to gather environmental

visual information and detect targets of interest, which requires first an optimal visual field (Martin, 2017). The visual field encompasses the volume of space surrounding the head from which visual information can be gathered at any given moment. The fields of view vary significantly among bird species, and are associated with different foraging, parental care, predator detection and sociality (Martin, 2017). However, the visual field is in trade-off with other visual abilities needed for spotting, such as spatial resolution. For instance, Old World passerine birds (Emberizidae) with a large binocular overlap - the area seen by both eyes simultaneously - typically exhibit low spatial resolution (Moore et al., 2015). Eye size is generally a strong predictor of visual acuity in birds (Kiltie, 2000). Predatory and scavenging species from open habitats typically have larger eyes, resulting in higher spatial resolution (Caves et al., 2024). In addition to spatial resolution, target detection requires the ability to discern contrasts (*i.e.* contrast sensitivity). Generally, birds have relatively low contrast sensitivity (Blary et al., 2024). Phylogeny tends to explain around 25% of variation in birds (Blary et al., 2024), suggesting that other factors such as foraging behaviour may be a driver of contrast sensitivity. When a target is in movement, the temporal resolution is also an important component for detection, which can vary over 3 degrees of magnitude among species (Potier et al., 2020a).

Finally, differences in photoreceptor spectral sensitivity among bird species are shaped by a combination of ecological drivers such as diel activity patterns (Wu et al., 2016), foraging strategies (Odeen & Håstad, 2010, Wu et al., 2016), sexual selection, predator-prey interactions or social signalling (Outomuro et al., 2017, Cooney et al., 2019). Collectively, these factors contribute to the evolution of diverse, specialized visual systems finely tuned to each species' natural history, ecological niche and ethology. In particular, bird retinas are lined with light-detecting cells of multiple types: one type of rod photoreceptor and five types of cones including four types of single cone–each expressing distinct visual opsin pigments to support tetrachromatic vision– and one type of double cone, which plays a role in achromatic vision. Rhodopsin (Rh1) is mostly expressed in rods–the vertebrate photoreceptor type adapted to detect dim-light levels– and is especially abundant in nocturnal birds (Potier et al., 2020b). Cone opsins, on the other hand, predominate in the retina of diurnal birds, enabling spectral resolution across a wide range of wavelengths and typically confer tetrachromatic colour vision in the majority of species investigated to date (Kelber, 2019, Wu et al., 2016). Additionally, double cones make up 40-50% of the cone population in the retina and both members contain the same long wavelength-sensitive opsin (LWS) (Hart, 2001, Günther et al., 2021).

Molecular variation among opsin subtypes contributes to species-typical maximal spectral sensitivities (λ_{max}) (Hauser & Chang, 2017, Hagen et al., 2023). In addition, interspecific molecular tuning within each opsin subtype further enhance differences in visual pigment sensitivities (Frentiu & Briscoe, 2008, Carvalho et al., 2007, Aidala et al., 2012, van Hazel et al., 2013, Hauser et al., 2014). Bird short-wavelength opsins type 1 (SWS1) occur in two types, ranging in maximal spectral sensitivity from near ultraviolet (300-400 nm) to violet (400-430 m) part of the spectrum (Hunt et al., 2007, Carvalho et al., 2007, Carvalho et al., 2011, Hauser et al., 2014). Given the significance of UV signalling in visual ecology, research on short-wavelength sensitivity has focused on identifying evolutionary trajectories and unique molecular mechanisms in vertebrates. This work revealed several spectral residues that contribute to expanding the bird SWS1 absorption spectrum across the UV-Violet range (Hart & Hunt, 2007, Hauser et al., 2014, Hagen et al., 2023). Short wavelength opsins type 2 (SWS2) typically absorb maximally between 430 and 460 nm, middle wavelength sensitive opsins (MWS or Rh2) absorb light in the range 470-510 nm, and long wavelength (LWS) opsins subtypes absorb light between 530 and 560 nm. Bird cones, alike those of lizards and turtles (Borges et al., 2015, Corredor et al., 2022, Hagen et al., 2023) contain carotenoid-rich coloured oil droplets functioning as short-wavelength cut-off light filters, which can modulate the associated photoreceptor spectral sensitivity of single cones generally shifting peak sensitivity to longer wavelengths (Hart, 2001, Knott et al., 2010, Toomey et al., 2015, Lim & Pike, 2016).

Identifying and integrating species-specific optical, behavioural and molecular characteristics of bird visual systems can reveal subtle differences that contribute to confer finely tuned adaptations involved in a species ecology. These insights may then inform on a system's physical or physiological limitations that may affect visually guided behaviours in a variety of natural and man-made environments. For example, collisions against wind turbines and power lines represent a major source of mortality caused by human activities (Marques et al., 2014, Bernardino et al., 2018). Additional sources of collision lies in the creation and expansion of infrastructure related to ski areas, including ski lifts and cables, and other developments such as urbanization and transport systems (e.g., cable cars, surface lifts, and Catex systems), which have been identified as a major cause of population decline in mountain birds (Buffet & Dumont-Dayot, 2013). Studying the visual system and behaviour of birds can help inform strategies to reduce this negative impact (Martin, 2011a, Martin, 2022, Martin & Banks, 2023).

Among European mountain birds, the black grouse *Lyrurus tetrix* (Galliformes: Phasianidae) account for up to 70% of bird mortality due to collision, notably in the French alps

(Buffet & Dumont-Dayot, 2013). This represented no less than 476 individuals in an earlier 4-year survey (Bech et al., 2012), a high figure which is likely an underestimate. To reduce collisions, a number of bird diverters have been developed, with varying efficiency depending on the type and bird species (Ferrer et al., 2020). Moreover, measuring their effectiveness is particularly challenging on mountain infrastructure. One reason for this may be that bird diverter designs have been based primarily on human perception and engineering considerations (Martin, 2022), rather than on the perceptual abilities of birds themselves. Therefore, it is crucial to understand specific visual behaviour and perception abilities of species subjected to collision risks, as it could contribute to design more effective visual diverters and improve conservation efforts in natural habitats.

In this study, we used an integrative approach and range of experimental techniques to determine the visual abilities of the black grouse and better understand its visual system's requirements to detect objects. We analysed reflex-like and ophthalmoscopic behaviours to characterize different components including the visual field, spatial resolution and contrast sensitivity. We then used RNA sequencing (RNA-Seq) to profile opsin genes in the retina and determined the spectral sensitivities of SWS1, SWS2, MWS and LWS opsins through heterologous expression and UV-Vis analyses. Finally, we integrate morphological, experimental and molecular analyses to define visual diverters detectability, taking into account visual constraints such as the role of oil droplets on spectral sensitivity. Altogether, our results provide a more comprehensive analysis of the black grouse visual abilities to better inform conservation initiatives.

Material and methods

(a) Visual field

(i) Birds and study location

Two 4-month-old male black grouse (*Lyrurus tetrix,* Phasianidae) individuals belonging to the breeding centre of Frank Grosemans (Belgium) were used to study contrast sensitivity. The experiments were run on site on October 5, 2022.

(ii) Experimental procedure

We used a non-invasive procedure to measure visual field characteristics in alert birds,

described previously (Fernandez-juricic et al., 2008, Martin, 2007, Potier et al., 2016b, Potier et al., 2017b). Each bird was held firmly for 20-30 min in a plastic restraining tube of the appropriate size to avoid any movement. The bird's legs were gently immobilized with light tape (Micropore Surgical tape 1530/1B) together and cushioned by foam rubber held between them. The head was held at the centre of a visual field apparatus (a device that permits the eyes to be examined from known positions around the head) by a specifically manufactured steel and aluminium bill holder. The head was maintained in the visual field apparatus following the natural head position of the birds. The surfaces of the bill holder were coated in cured silicone sealant to provide a non-slip cushioned surface. We held the bill in place with Micropore tape, ensuring not to cover the nostrils to allow for normal breathing. We took calibrated photographs (Iphone 13, Apple) of the head and the eyes of each bird while held in the apparatus to determine eye positions within the skull, the horizontal separation between the centre of the two eyes, the distance between the centre of the eye and the bill tip, and the bill length.

Visual field parameters were measured using an ophthalmoscopic reflex technique. The perimeter's coordinate system followed conventional latitude and longitude measures, with the equator aligned vertically in the median sagittal plane of the head (i.e., a vertical plane that divides the head symmetrically into left and right hemisphere). We used this coordinate system in the presentation of the results. We examined the eyes using an ophthalmoscope mounted against the perimeter arm with an accuracy of ± 0.5°. We measured the boundaries of the retina projection by the positions that the eyes spontaneously adopted when they were fully rotated 'forwards' (converged for estimation of binocular area boundaries) and 'backwards' (diverged for estimations of the blind sectors boundaries) for the blind area behind the head. We did not measure the degree of eye movements or the projection of the pecten to reduce the time the animals were restrained.

We corrected our data for viewing from a hypothetical viewing point placed at infinity. This correction is based upon the distance used in the measurements taken with the visual field apparatus and the horizontal separation of the eyes (Martin, 1984). After the corrections, we constructed a topographical map of the visual field and its different components. These features included lateral fields, binocular field, cyclopean field (the total field around the head produced by the combination of the monocular fields of both eyes), and blind areas above and behind the head. The limits of the visual field were determined at 10° intervals of elevation in an arc from directly behind the head, to above the head, and then down to 50° below the horizontal in front of the head. We did not record data at elevations where the bill holder was blocking our view

and instead estimated the binocular field width as the mean value of the binocular field widths immediately above and below these elevations (Martin, 2017).

(b) Eye size and visual acuity

We estimated the spatial resolving power of the eye based on Corneal Diameter (CD) from the calibrated photographs (Spiegel et al., 2013, Potier et al., 2016a, Potier et al., 2017b) Corneal diameters were measured with ImageJ 1.41 (Schneider et al., 2012) and then translated to Axial Length (AL) using the formula for diurnal animals (Hall & Ross, 2007):

$$AL = \frac{CD}{10^{-0.22}}$$

We then calculated the spatial resolution (SR) using the following function derived from (Caves et al., 2024):

$$SR = 10^{(0.26 + 0.81 * log_{10}(AL))}$$

(c) Contrast sensitivity

(i) *Lyrurus tetrix* birds and study location

Experiments were performed on October 6, 2022 on the same individuals used in experiment (a) at the breeding centre of Frank Grosemans (Belgium).

(ii) Experimental set-up

We used a reflex-like behaviour setup to study the contrast sensitivity of each individual, following Wagner et al. (2022) and Blary et al. (2024). This approach yields peak contrast sensitivities similar to those obtained with the operant conditioning method (Blary et al., 2024) but not the associated spatial frequency. These reflexes or nystagmus are caused by involuntary compensatory mechanisms for image stabilization, *i.e.,* the individual follows the moving object by eyes to keep the image stationary on the retina (Wagner et al., 2022). Because most birds have limited eye movements (between 2 and 18°) (Martin, 2009, O'Rourke et al., 2010), they follow the object with large head movements. To estimate the optocollic reflex (OCR), birds were placed into a U-shaped box adapted to the size of the species (60 x 40 x 44 cm ; L x

W x H), with a black wooden floor and ceiling, and clear polycarbonate walls (3 mm). The walls allowed the bird to see the stimulus, without influencing visual abilities (Blary et al., 2024). The ceiling was made of two wooden boards spaced 5 cm apart: a perforated panel to let the air pass through and a solid and smaller panel so that the bird could not see through the holes of the other panel. All wooden surfaces were painted matte black (Liberty black Matt, GoodHome). A wooden door placed at the back of the box allowed to position the bird in the box. The experimental box was placed at the centre of an octagon of a radius of 69cm made of computer monitors (Acer KG1 Series, 28 inches (62x34 cm), 4K 3840x2160 pixels, 60 Hz, Acer Inc. Taiwan), in portrait orientation, with the centre placed on the same level as the bird's head. The stimulus covered 236x46 degrees of the visual field (horizontal x vertical extent). This layout covered enough of the bird's visual field to elicit an OCR (Schmid & Wildsoet, 1998, Blary et al., 2024).

The monitors and the bird were placed in an opaque black cloth tent (300 x 300 x 250 cm; L x W x H) with the base of monitors and the floor also covered by an opaque black cloth to minimize possible disturbing external visual signals. The experimenter stayed outside the tent during the entire duration of the experiment. One video camera (25 frames per second; Sony DCR-SR55 HD) placed above the monitors, allowed recording the bird's behaviour during the experiment. In addition, a smartphone (Iphone 13, Apple) connected to a screen located outside the tent was used so that the experimenter could monitor the bird during the entire procedure.

(iii) Stimuli

The stimuli were generated in Matlab (R2021) using Psychtoolbox (Brainard, 1997). The computer monitors were connected to a MacBook Pro (Apple) using a HDMI splitter (8-Port, 4K, 60Hz, ST128HD20, StarTech). The stimuli comprised vertical sinusoidal achromatic gratings with varying spatial frequencies and contrasts. The angular velocity was set at 20 degrees per second, similar to values used for closely related species (Blary et al., 2024). To obtain the contrast sensitivity function (CSF), *i.e.* the peak contrast sensitivity along with the corresponding spatial frequency and the high cut-off frequency (*i.e.* the highest SF perceived by the individual at a Michelson contrast of 1), we used six spatial frequencies (0.47, 0.56, 0.85, 1.06, 1.27 and 1.59 cycle per degree (c/deg)) and Michelson contrast ranging from 0.012 and 0.99 (Table S1). Specifically, Michelson contrast is defined as:

$$Michelson\ contrast = \frac{I_{max} - I_{min}}{I_{max} + I_{min}}$$

where I_{min} and I_{max} represent the highest and lowest luminance. For each contrast level tested, the contrast was evaluated with a luxmeter (Hagner ScreenMaster, B. Hagner, Sweden) by measuring the difference in luminance between the darkest and lightest area of the grating at the centre of the monitor and expressed in candelas per square meter (cd/m^2).

Each stimulus was shown on monitors for 20 seconds (Schmid & Wildsoet, 1998, Shi & Stell, 2013, Wagner et al., 2022, Blary et al., 2024). The direction of the stimulus (clockwise or anticlockwise) was changed in a pseudo-random order, *i.e.* the number of consecutive trials in the same direction was limited to three. The illuminance at the bird's head was measured with the luxmeter: 110 lux inside the U-shaped box and 321 lux outside. The stimulus brightness was 73 cd/m^2.

(iv) Experimental procedure

Computer monitors were turned on 20 minutes before the beginning of the experiment so that they reached maximum brightness. The experimental session began after a 10-minute habituation period following the bird's placement in the device. The experimenter visually assessed the presence of OCR, following standard practice (Schmid & Wildsoet, 1998, Shi & Stell, 2013, Blary et al., 2024). Each session began with maximum contrast (i.e. Michelson contrast = 0.99) to ensure that the bird was expressing an OCR detectable by the experimenter. The contrast was then decreased and increased in a robust stepwise manner as described in Blary et al. (2024) to approach the contrast threshold where birds no longer exhibited the reflex. Each trial consisted of a specific combination of spatial frequency and contrast, separated by at least 5 seconds during which an isoluminant homogeneous grey was displayed on monitors (longer pause if the bird did not look at the monitors). We used the "four of five" criteria, *i.e.* each specific combination was presented 5 times and the response was considered reliable if the OCR was elicited at least 4 times out of the 5 trials (Shi & Stell, 2013, Blary et al., 2024). Thus, the lowest contrast within a validated 4/5 criterion was defined as the threshold contrast. Once this threshold was reached, the experiment was repeated with the same angular velocity but with a different spatial frequency. Since each session was video recorded, the experimenter could review the trials retrospectively, confirm the presence or absence of OCR and use the results from double-checked blind results for the analyses.

(d) Opsin spectral sensitivity

(i) Collection of eye tissues and extraction of ribonucleic acid (RNA).

Ocular tissue, including the retina, was dissected by a veterinarian from an accidented adult female black grouse *L. tetrix,* collected in Bourg-Saint-Maurice France (ID: JB-2021-E001, POIA Birdski Project 2020-2023 Vanoise), respecting permits in place. The collected tissue was directly preserved in DNA/RNA reagent (Zymo Research) and stored at -20° C. Before extraction, the tissue sample was removed from the stabilization solution, briefly dried and then ground to a fine powder in a mortar cooled with liquid nitrogen. We then proceeded with RNA extraction with a Monarch Total RNA miniprep kit (NEB) following the manufacturer's instructions. The integrity of the RNA was evaluated using a bioanalyzer and the quantity assessed using a Qubit High Sensitivity RNA assay (Invitrogen).

(ii) cDNA libraries and RNA-sequencing.

Five hundred micrograms of high-quality RNA were used to prepare a deoxyribonucleic acid (DNA) library following the protocol detailed in NEBNext Ultra II Directional RNA library prep kit for Illumina (NEB), including the following specifications: selection of messenger RNA (mRNA), a selected average size of 500 base pairs for fragmentation, and the addition of Illumina adapters. The quality of the cDNA library was evaluated using a bioanalyzer as well as by quantitative PCR (Polymerase Chain Reaction). Paired-end sequencing (2x150bp) was performed on an Illumina NovaSeq6000 equipped with an S4 flowcell (NovaSeq Control Software 1.8.0/RTA v3.4.4, SciLifeLab, Stockholm, Sweden). In total, we obtained 197.8 million read pairs. The transcriptome sequencing data have been deposited into the European Nucleotide Archive (ENA) under the project accession PRJEB86944.

(iii) Pre-assembly filtering

Raw reads were first preprocessed by correcting and excluding aberrant reads using the k-mer-based read-error correction tool Rcorrector (Song & Florea, 2015). We next proceeded to adapter removal and quality trimming (--quality-cutoff=20) using cutadapt version 4.2 (Martin, 2011b). During that step, we also removed read pairs with either read shorter than 36 bp. Next, we removed reads corresponding to rRNA sequences by mapping the reads against a custom database built from SILVA SSU and LSU datasets (release 138.1) (Quast et al., 2013) using bowtie2 (Langmead & Salzberg, 2012). Finally, reads corresponding to mitochondrial sequence

were extracted using MITGARD (Nachtigall et al., 2021). The final set of assembly-ready reads contained 173.8 million read pairs.

(iv) *De novo* transcriptome assembly and annotation

De novo assembly of the pre-processed paired-end reads was performed using Trinity v2.14.0 (Grabherr et al., 2011) with default parameters. Completeness of the assembly was assessed with BUSCO v3.0.2 (Simão et al., 2015) using the Vertebrata and Aves datasets. We applied the pipeline implemented in Trinotate v3.2.1 (Bryant et al., 2017) to predict candidate protein coding regions within transcript sequences using TransDecoder v5.5.0 (https://github.com/TransDecoder/TransDecoder) and to generate a functional annotation of the transcriptome data. We retrieved full-length candidate opsin transcripts from the resulting annotation table (Dataset S1).

(v) Expression estimates

We obtained expression estimates using RSEM v1.3.0 (Li & Dewey, 2011). First, we generated a transcript to gene mapping file from the Trinity output using the dedicated script from the RSEM package. Next, quality-trimmed paired-end reads were aligned to the transcriptome using Bowtie2 v2.4.1 (Langmead & Salzberg, 2012). The overall alignment rate was 85.29%. Finally, RSEM was used to compute the expression estimates.

(vi) Opsin functional expression

Opsin-specific oligonucleotide primers (Table S2) encompassing two distinct restriction sites were designed to amplify the coding region of each identified visual opsin (SWS1, SWS2, Rh2, LW) by PCR using retinal cDNA synthesized using the GoScript protocol (Promega) as template. After verification by agarose gel electrophoresis, expected amplified product sizes were gel-purified using the Monarch DNA gel extraction kit (NEB), digested with restriction enzymes, subcloned into the linearized pcDNA5-FLAG-T2A-mruby2 expression vector (Liénard et al., 2021), and propagated into a Q5 strain of *Escherichia coli* bacteria (NEB). After incubation of individual bacterial colonies in Luria-Broth culture medium containing ampicillin, DNA plasmids were purified, and each construct sequence was verified by Sanger sequencing. A stock of each final plasmid was prepared following the ZymoPURE II Plasmid MidiPrep kit protocol (Zymo, D4200) to obtain a quantity of 480 micrograms.

(vii) Protein purification, absorbance measurement and UV-VIS analyses

Each plasmid was transfected into human embryonic kidney cells (HEK293T) following the PASHE procedure (Liénard et al., 2022). Briefly, 11-*cis*-retinal was added in solution in the dark (under red light) 6h post transfection. Cells were collected and the total membrane fraction solubilized using n-Dodecyl-D-Maltoside detergent (DDM) 48h after transfection, and the opsin fraction bound to FLAG resin and incubated overnight. The next day, the opsin-FLAG complex was purified and eluted using FLAG peptide, subsequently concentrated by centrifugation at 4000 rpm and 4°C for 50 min prior to ultraviolet-visible (UV-VIS) spectroscopy. The purified rhodopsin (opsin in complex with the chromophore) was dark-adapted in solution and its absorbance was measured in the dark from 1.5 µL aliquots using a NanoDrop 2000/2000c UV-VIS spectrophotometer (ThermoFisher). For each rhodopsin, we estimated lambda max by nonlinear fitting of the absorbance data using a visual pigment template (Govardovskii et al., 2000). We performed 1,000 bootstrap replicates to compute lambda max estimates and the associated confidence intervals (Liénard et al., 2022) in R v. 3.6.6. using the rsample (Frick et al., 2022) and tidymodels (Kuhn & Wickham, 2020) packages.

Results

(a) Black grouse visual field

The maximum binocular overlap was 40°, positioned 30° above the eye bill-tip direction (Figure 1). At rest, black grouse have a binocular overlap of 28° and a blind spot of only 7° behind the head (Figure 1). The vertical extent of the binocular field in the median sagittal plane was 170° and extended 40° behind from directly above the head to the horizontal (Figure 1). The binocular field width from directly above the head to the horizontal was 6°. Lateral placement of the eyes in the skull, coupled with wide monocular fields and small blind spot provides a large cyclopean field, i.e. the full extent of the volume of space around the head that at any one instant can provide visual information.

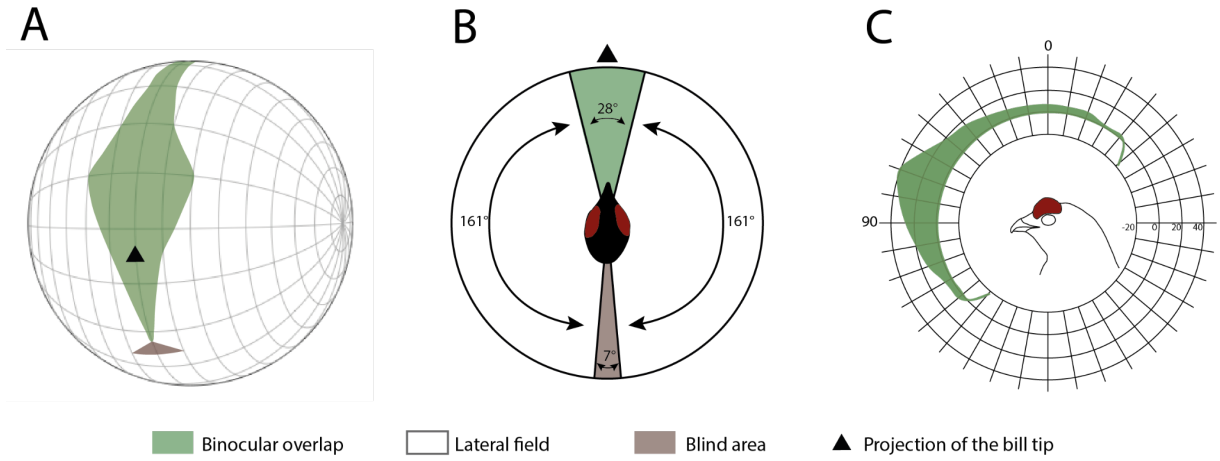

Figure 1. Visual fields of the black grouse. (A) Orthographic projection of the boundaries of the retinal fields of the two eyes. A latitude and longitude coordinate system was used with the equator aligned vertically in the median sagittal plane. The bird head is imagined to be at the centre of the globe with a grid at 20° intervals in latitude and 10° intervals in longitude. (B) Horizontal section through the horizontal plane (90-270°) showing the extent of the binocular overlap, lateral fields and blind spot in black rouse. (C) Binocular field as a function of elevation in the median sagittal plane. Orientation of the bird head is shown diagrammatically. All values are in degrees and the grid is at 10° intervals. Each chart represents the average retinal visual field when the eyes were converged (of the two individuals). Green areas represent the binocular sector, white areas the monocular sectors and brown areas the blind sectors.

(b) Contrast sensitivity and visual acuity

Contrast sensitivity is dependent on the spatial resolution of the stimulus and is expressed as the inverse of Michelson contrast. We found a maximum contrast sensitivity of 16.67 for both

individuals at a spatial frequency of 1.06 cycle per degree (cpd; Figure 2). Individual B had a similar contrast sensitivity value at 0.85 cpd as well. This sensitivity corresponds to Michelson contrast of 6%. The extrapolated spatial resolution at highest contrast (contrast sensitivity = 1) was around 1.6 cpd.

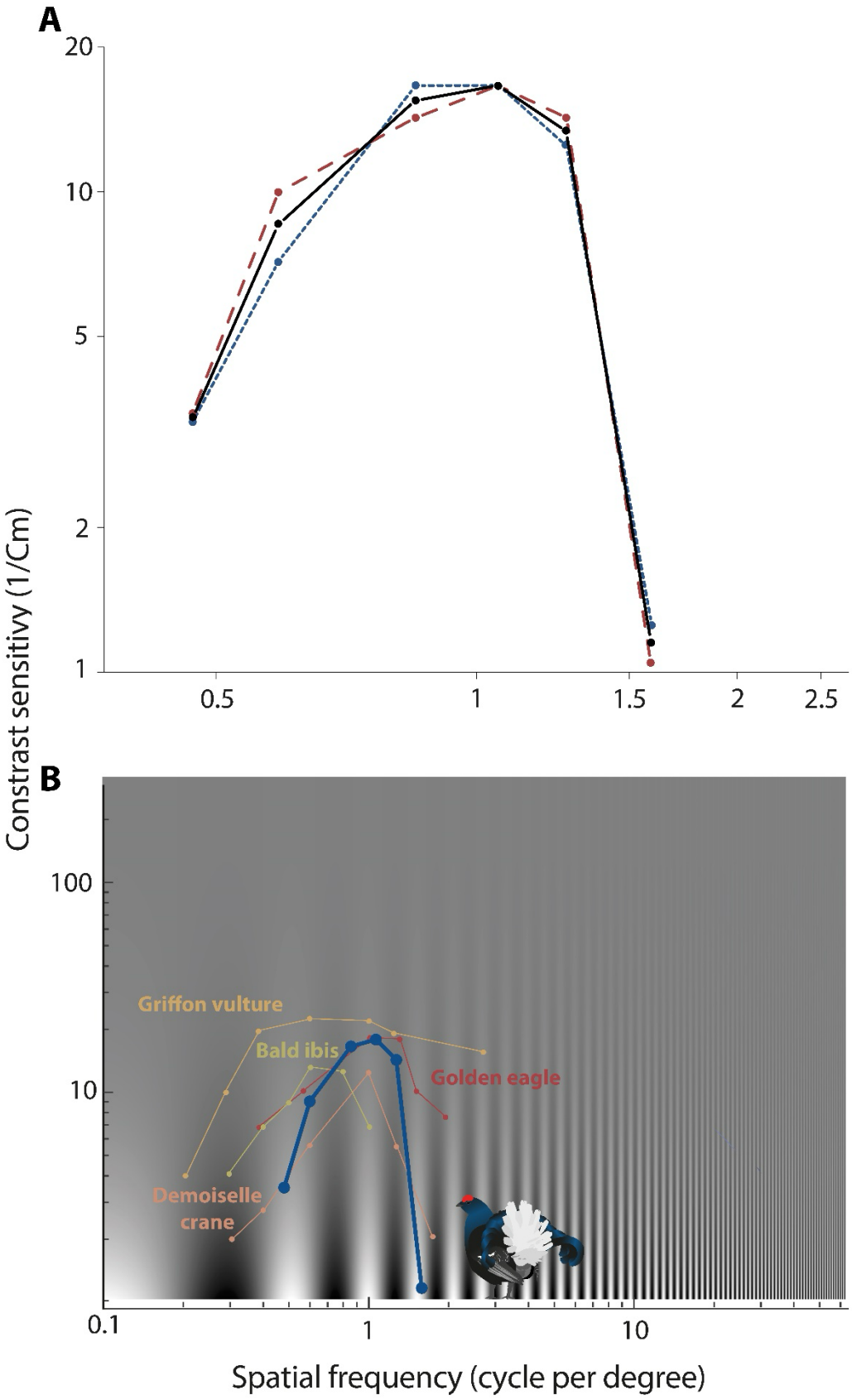

Figure 2. Contrast sensitivity of the black grouse, defined as the inverse of contrast threshold, as a function of spatial frequency. (A) Coloured and dashed curves are individual values, while the black

curve represents the pooled data. Note that the scales of the axes are logarithmic. (B) Comparison of the contrast sensitivity of the black grouse (blue) and selected species. Note that the scales are logarithmic.

The measured Corneal Diameter (CD) from close-up photographs was 8.00 mm for both individuals. The estimated Axial Length (AL) was therefore 13.28 mm, which corresponds to a spatial resolution of 9.81 c/deg.

(c) Opsin spectral sensitivity

To determine the spectral sensitivity of cone opsins expressed in retinal photoreceptors of the black grouse, we first carried out a transcriptomic profiling to identify opsins mRNAs expressed in the retina and determine their phylogenetic placement (Dataset 1). Our analyses revealed 4 transcripts corresponding to known classes of bird visual cone opsins belonging to the short wavelength (SWS1 and SWS2), medium wavelength (MW or Rh2), and long wavelength (LW) subfamilies, as well as the dim-light sensitive rod opsin (Rh1), which is associated with achromatic rod vision and has a conserved maximum absorbance of ~500 nm.

Open reading frame sequences for cone opsins were subcloned into a modified pcDNA5-FLAG-T2A-mruby2 expression cassette and the resulting plasmid construct was transiently expressed in HEK293T cells. Active rhodopsin complexes were reconstituted in vitro by addition of 11-*cis*-retinal, after which rhodopsin proteins were isolated from cell membranes and purified using FLAG resin affinity binding following Liénard et al. (2022). Concentrated rhodopsin eluates were analysed by ultraviolet-visible spectroscopy to determine the absorbance profiles of each opsin type. These analyses showed that the SWS1 and SWS2 opsins absorb maximally at λ_{max} of 393 ± 2nm (Figure 3A), and λ_{max} of 436 ± 3nm (Figure 3B), respectively. We then measured the absorbance of black grouse Rh2 and LW, which displayed maximum sensitivity to light at 482 nm ± 2.5 nm (Figure 3C) and 545 ± 2.5 nm (Figure 3D), respectively.

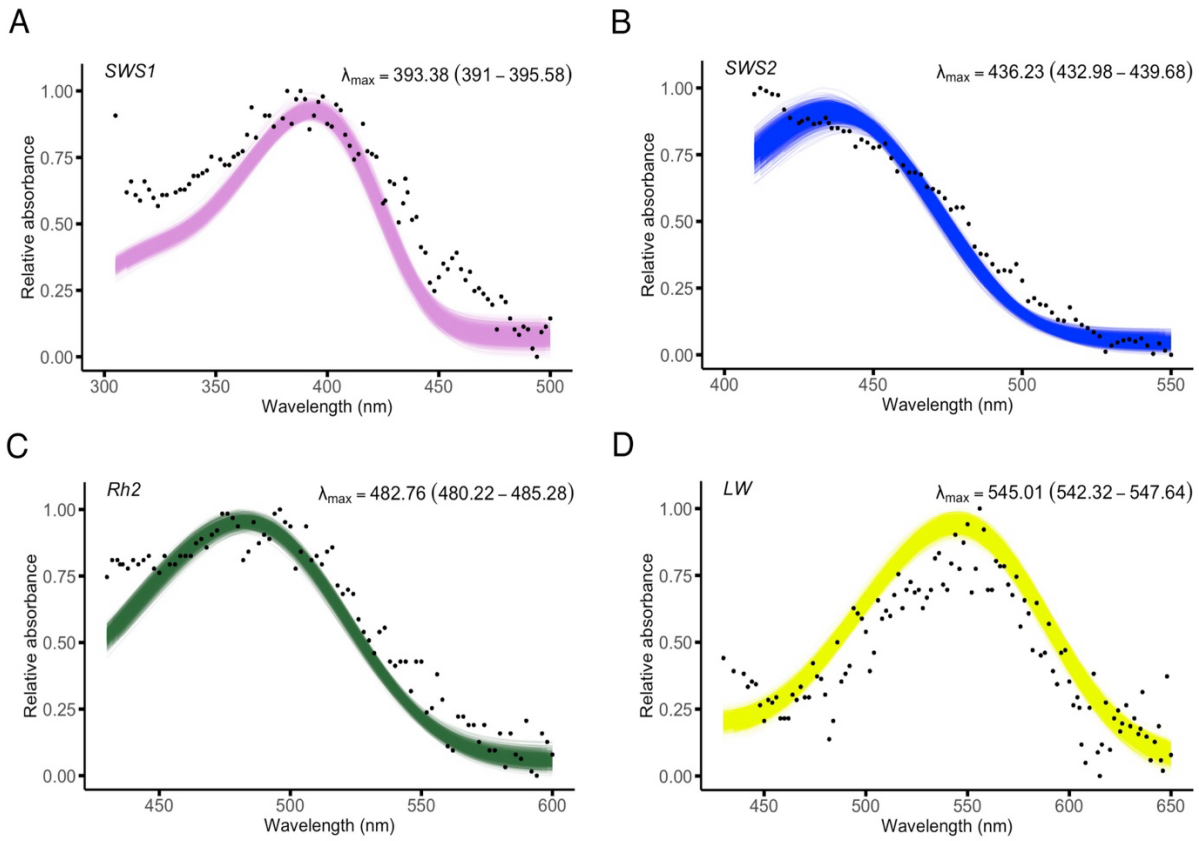

Figure 3: Functional expression of *Lyrurus tetrix* visual cone opsins. Absorbance curves (A-D) of visual rhodopsins reconstituted in presence of 11-*cis*-retinal and purified from HEK293T cells. The black dots represent the average absorbance across replicates at every wavelength, whereas the lines represent the curve-fitting of individual bootstrap replicate. (A) SW1 (n = 7), (B) SW2 (n = 6), (C) Rh2 (n = 3), (D) LW (n = 7), where n is the number of measurements of protein aliquots with active rhodopsin complexes. For each rhodopsin, relative absorbance data are fitted to a visual template with polynomial function analyses computed in R to obtain the estimates of lambda max following 1,000 bootstrap replicates (Liénard et al., 2022). Values in parentheses represent the 95% confidence intervals lower and upper bounds. Accompanying data are provided in dataset S2.

Overall, the four visual opsins confer broad wavelength sensitivity from 300 to 650 nm (Figure 3; Figure 4A). Based on the measured spectral sensitivity of SWS1, we calculated the predicted theoretical cut-off value of C-type oil droplets in SWS2 cones following Hart (2001), which falls at approximately 430 nm (predicted cut-off C-type droplets; Figure 4B). Our analysis indicates that the black grouse SWS1 is a violet sensitive pigment, with near ultraviolet sensitivity (Figure 4C).

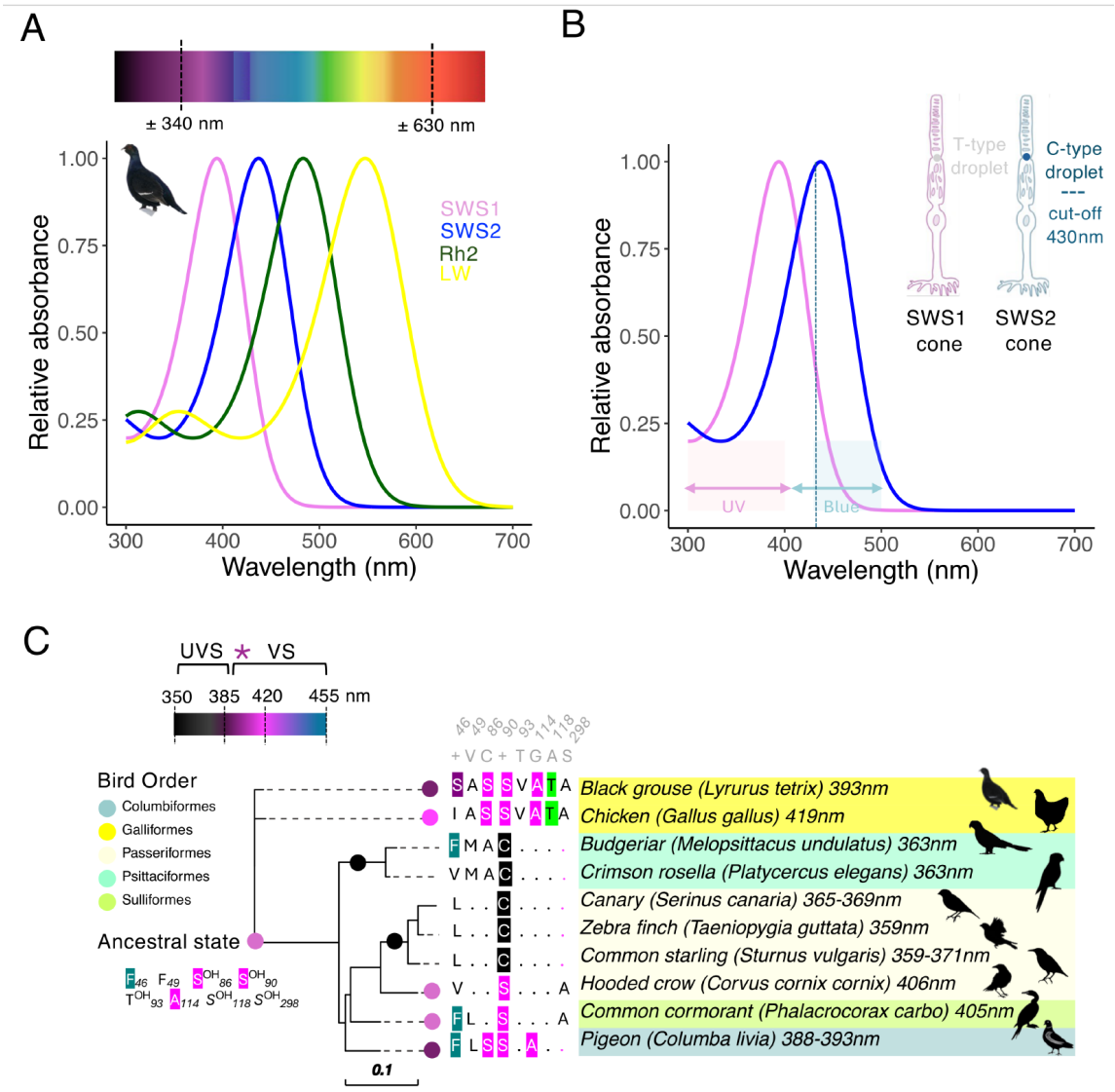

Figure 4: **Opsin spectral sensitivity curves in the black grouse, *Lyrurus tetrix* and its light perception**. (**A**) Spectral sensitivity curves for SWS1, SWS2, Rh2 and LW visual cone opsins confer broad light perception in the range 340 to 630 nm. (**B**) The presence of C-type droplets in bird SWS2 cones affects the perception of ultraviolet light, and a cut-off value can be predicted based on the maximal sensitivity of the SWS1 opsin (Hart, 2001), which for *Lyrurus tetrix* would be projected at 430 nm, indicating that the SWS2 cone would not absorb wavelengths shorter than 430 nm (dashed blue line). The SWS1 cones have transparent T-type oil droplets that do not absorb light, and thus the SWS1 cone would absorb UV light. (**C**) SWS1 opsin phylogeny of selected bird species where SWS1 opsin lambda max (λ_{max}) determined experimentally is indicated after the species name. Letters represent amino acid residues known to be important for SWS1 maximal sensitivity, and the numbers represent their position relative to the bovine rhodopsin (Acc. Number AAA30674). OH refers to amino acids bearing a hydroxyl group. Dots in the alignment correspond to a conserved residue with the consensus sequence in grey. The asterisk positions the black grouse SWS1 as a violet sensitive pigment, with near ultraviolet sensitivity. UVS, ultraviolet sensitivity; VS, violet sensitivity.

Discussion

The visual system of the black grouse indicates a relatively low spatial resolution and contrast sensitivity but a high visual coverage for birds

The black grouse showed a high visual field coverage but relatively low contrast sensitivity and visual acuity, visual characteristics that are typical of prey species (Martin, 2017). In birds, binocularity is thought to function primarily in the detection of symmetrically expanding optic flow-fields that provide almost instantaneous information on the direction of travel and time-to-contact a target (Martin, 2009, Martin & Portugal, 2011). The maximum width of the frontal binocular field was 28° and fell well within the range of other birds (20-40° on average) (Martin, 2017). Maximum binocular field width was found to be 30° below the eye bill-tip direction, similarly to other species that forage on the ground by vision such as the Southern caracara *Caracara plancus* (Potier et al., 2017a). Therefore, it seems very likely that the binocular field of the black grouse represents an adaptation to its foraging technique, as found in many similar bird species (Martin & Portugal, 2011, Potier et al., 2018, Cantlay et al., 2023, Potier et al., 2023).

The results on the visual field configuration of the black grouse also showed that this species has an exceptionally extended visual field in both the horizontal and vertical planes. To date, on more than 150 species studied, only 4 species had a smaller blind spot behind the head (3 ducks: the Mallard *Anas platyrhynchos*, the Northern pintail *Anas acuta* and the Pink-eared duck *Malacorhynchus membranaceus*) (Martin, 1986, Guillemain & Fritz, 2002, Martin, 2007), as well as the Eurasian woodcock *Scolopax rusticola* (Martin, 1994). This configuration allows the black grouse to gain a comprehensive visual coverage of the celestial hemisphere. Black grouse adopting the typical head position depicted in Figure 1 can thus gather visual information from above the head without the need of head movements. This would allow foraging and predator detection to be conducted almost simultaneously. It is however important to note that in this species, the presence of the suborbital feathers ridge in male may reduce the visual coverage compared to females, as found in other Galliformes species (Lamond et al. in press).

While eye size correlates with visual field parameters in birds, such as blind spot above the head (Martin, 2007), larger eyes also confer higher visual acuity (Kiltie, 2000, Caves et al., 2024). The estimated visual acuity of the black grouse is relatively low compared to predatory species but similar to most prey species (Martin, 2017, Caves et al., 2024). Furthermore, our estimation of visual acuity based on eye size (i.e. 9.81 cycle per degree) is very similar to closely related species from the same order Galliformes (based on 7 species, ranging from 9.7 c/deg for

the Japanese quail *Coturnix japonica* to 13 c/deg for the Sharp-tailed grouse *Tympanuchus phasianellus* (Lisney et al., 2012). High visual acuity is not necessary for ground-foraging birds (Potier et al., 2016a), thus, there may be limited selection pressure for increased spatial resolution in black grouse.

Finally, the maximum contrast sensitivity of the black grouse (i.e. 16.67) is similar to other birds tested so far, ranging from 4.8 for the Bourke's parrot *Neopsephotus bourkii* to 31 for the American kestrel *Falco sparverius* (Hirsch, 1982, Lind et al., 2012, Blary et al., 2024). The contrast sensitivity of the black grouse is therefore 4.5 to 10.5 times lower than large mammals (Bisti & Maffei, 1974, De Valois et al., 1974, Merigan, 1976, Jacobs, 1977, Langston et al., 1986) but similar to small mammals such as rats (Birch & Jacobs, 1979, Keller et al., 2000). It is not fully understood why birds have relatively low contrast sensitivity. One possible reason could be a trade-off between contrast and colour sensitivity (Ghim & Hodos, 2006). Indeed, most birds perceive more colours than the majority of mammals (Hart, 2001), and some can perceive colours at greater distances (Potier et al., 2017a). In black grouse, the presence of a fourth type of cone sensitive to very short wavelengths near the ultraviolet region may be potentially energetically costly (Niven & Laughlin, 2008). Hence, in mammals, species sensitive to UV light, such as rats, have lower contrast sensitivity than species that are non-sensitive to UV light, such as primates (De Valois et al., 1974, Merigan, 1976, Jacobs, 1977, Birch & Jacobs, 1979, Langston et al., 1986, Keller et al., 2000, Hunt et al., 2001).

Opsin-based visual spectral sensitivity confers broad wavelength perception and presumably near-ultraviolet (UV) vision

There has been a long-standing interest in determining the possible role of ultraviolet light and spectral sensitivities at short wavelengths in animal vision, in the context of intra- and inter-specific signalling but also foraging abilities across animal groups, including in invertebrates (Cronin & Bok, 2016, McCulloch et al., 2017, Finkbeiner & Briscoe, 2021); terrestrial vertebrates including snakes (Crowell et al., 2024), lizards (Pérez i de Lanuza & Font, 2014) and birds (Massaro et al., 2003).

In particular, avian and mammalian SWS1 visual pigments exhibit a broad natural variation from very short UV sensitivity to violet sensitivity and have been studied at the molecular and *in silico* level in relatively great details (Hunt et al., 2009, Hauser et al., 2014, Yokoyama et al., 2016, Patel et al., 2018). The four cone opsins (SWS1, SWS2, Rh2 and LW) characterized from the black grouse retina and reconstituted *in vitro* via heterologous expression

showed maximal peak sensitivities at 393 nm (SWS1), 436 nm (SWS2), 482 nm (Rh2), and 546 nm (LW) (Figure 3). Our results align with observed spectral ranges across bird species investigated to date (reviewed in Hauser et al., 2014, Hagen et al., 2023), supporting that opsin-based spectral sensitivity confers light perception from ultraviolet (UV) wavelengths to very long wavelength light, from 340 to 650 nm (Figure 4).

The 393 nm sensitivity of black grouse SWS1 is an interesting intermediate between known very shifted UV sensitive and violet SWS1 bird pigments (Figure 4C). Several spectral tuning sites have been identified that contribute to expand the absorbance of SWS1 opsins from violet to shorter ultraviolet light (Figure 4C) (e.g. Hagen et al., 2023). In particular, , birds most likely ancestrally possessed a violet-sensitive SWS1 pigment, whereas ultraviolet sensitivity has been regained subsequently in certain lineages (Shi et al., 2001), allowing visual and ecological adaptations (Hauser & Chang, 2017, Hauser et al., 2014, Hagen et al., 2023). Also, the variability of avian SWS1 spectral tuning residues seems overall more consistent than residues regulating mammalian and other vertebrate SWS1 pigment sensitivity (Hauser et al., 2014), which can be explained to a large degree by amino acid convergence at specific sites (Figure 4C) (Hauser et al., 2014). Yet, it remains interesting to obtain more experimental *in vitro* expression data on additional SWS1 opsins, to further improve evolutionary inferences of extant UV/violet spectral sensitivity across the entire avian class. Although phylogenetically related to the chicken *Gallus gallus,* the Galliform black grouse has a SWS1 pigment absorbing in the near-UV (393 nm) similarly to the distantly related Columbiform pigeon *Columba liva* SWS1 pigment (Figure 4C) (Bowmaker, 1977). Although it is possible that small differences in measured spectral sensitivities for pigments purified *in vitro* may account for variations in experimental methods, several bird SWS1 have been shown previously to confer near-UV vision owing to measured properties of SWS1 pigments themselves, or *in silico* sequence predictions (Carvalho et al., 2007, Hauser et al., 2014). The black grouse exhibits many conserved spectral tuning sites of SWS1 with its close orthologue in the chicken yet exhibits a Serine residue at spectral tuning position 46 (Ser46), which may play a role in intermediate spectral sensitivity.

In many birds, the ocular media are UV transparent, especially in birds with UV-sensitive visual pigments (Lind et al., 2014) making sensitivity to UV wavelengths possible in cones expressing an ultraviolet-sensitive SWS1 visual pigment (reviewed in Cuthill et al., 2000). Colour vision in bird visual cones is however affected by distinct types of oil droplets that filter incoming light in the bird retina (Kelber, 2019). Cone oil droplets are positioned between incoming light and the cone visual pigments, acting as a filter which can influence the

pigment's effective spectral sensitivity by absorbing part of the incoming light spectrum. The oil droplet type in SWS1 cones is transparent (Hart, 2001) and leaves the opsin pigment intrinsic sensitivity. In SWS2 cones, the cone peak sensitivity is typically shifted to a wavelength longer than the opsin pigment inherent lambda max (Bowmaker, 1977, Olsson et al., 2017). This effect can be predicted based on SWS1 lambda max (Hart, 2001), overall reducing spectral sensitivity of SWS2 below 400 nm (Figure 4, Figure S9). Overall, oil droplets will thus reduce chromatic abilities while maintaining sensitivity to UV wavelengths (achromatic vision), owing to the black grouse SWS1 pigment function.

The behavioural role of UV vision in foraging has also been shown. If some UV wavelengths are present in the light environment, several bird species exhibit enhanced detection of UV reflecting food items. For instance, Church et al. (1998) showed that blue tits' foraging ability is enhanced by UV cues of cryptic caterpillars. Behavioural experiments showed the ability for several bird species, including redwing *Turdus iliacus* and black grouse (Siitari et al., 2002) to discriminate UV wavelengths. The black grouse shows a preference for European blueberries (*Vaccinium myrtillus*) reflecting UV owing to their natural wax coat compared to non-UV reflecting fruits (Siitari et al., 2002). Even if some part of the UV spectrum is likely filtered out due to typical oil droplets in bird SWS2 cones, not allowing true UV colour vision, black grouse still detect UV wavelengths and are sensitive even to low ultraviolet light intensities. Together, behavioural evidence with our opsin-based absorbance spectra results strongly support UV sensitivity in this species.

Recapitulating visual properties to inform vision-based collision mitigation

The visual capabilities of birds have been hypothesised as major cause of collision with man-made objects (Martin, 2011a, Martin, 2022, Martin & Banks, 2023). However, vision is a complex and multifaceted sense, underlying the necessity to explore different visual characteristics. In this study, we used an integrative approach by exploring black grouse visual fields, contrast sensitivity, eye size (and therefore visual acuity) and spectral sensitivity. All these visual capacities have been listed as essential in the context of collision, in addition to speed of vision and reaction time (Martin, 2022).

For instance, many birds fail to see the way ahead, such as large raptors from Accipitriformes (Martin et al., 2012, Portugal et al., 2017, Potier et al., 2018). Indeed, while searching the ground below for food, those raptors would gain no or intermittent information about the flight path ahead (Martin et al., 2012). This is especially true in familiar open habitats,

and when an unpredictable change occurs, such as human artefacts, that may lead to fatal collisions (Martin, 2022). We found that black grouse have an extended visual coverage, conferring them the ability to see the way ahead. Therefore, its visual field configuration itself should allow the birds to gather environmental information, for example the presence of an aerial object. This is interesting because it opens opportunities to optimize the visual perception of man-made objects by modifying the contrast (within the object or with respect to the background), colours, or using bird diverters for instance (Martin, 2022) to reduce the high number of collisions in this species.

In contrast to its extended visual coverage, the black grouse likely has a relatively low spatial resolving power (9.81 c/deg), which informs us at which distance they can detect objects in optimal conditions, including i) no air distortion and clear sky, ii) black object on a white background (i.e. high contrast scenario), iii) high daytime level, iv) the bird visually fixing the object with it acute centre of vision (Land & Nilsson, 2012, Martin, 2017, Martin, 2022). In this case, the distance at which an object is detectable and avoidable depends on the i) spatial resolving power, ii) time reaction and iii) flight speed. In birds, it is reasonable to assume a requirement of at least 2 seconds to take the action of changing flight path (Martin, 2022), although this prediction has to be confirmed by species-specific experimental validation. The typical flight speed of black grouse was calculated as 16.04 m.s-1 (35.88 mph) using the established relationship between body mass (1068.7g on average in black grouse (Dunning, 2007)) and flight speed (Alerstam et al., 2007). Therefore, giving a minimal estimated detection time of 2 sec, the shortest distance at which the black grouse can detect and avoid an object is 32m under optimal conditions. According to the estimated visual acuity, trigonometric calculations indicate that this object should be of a minimum size of $50mm^2$. However, in a natural scene, optimal conditions are rarely reached. Spatial resolution declines significantly with light level (Land & Nilsson, 2012), and a 5-fold decrease from maximum spatial resolution should be highly likely (Martin, 2022). In this case, the object should be 5 times larger, therefore of a minimum size of $250mm^2$. Because black grouse maximum contrast sensitivity, similarly to other birds, is relatively low, the internal object contrast, as well as the contrast between the object and its surrounding environment should be as high as possible (Martin, 2022). Also, under natural conditions, the range of background conditions against which an object appears is highly variable, and maximising internal object contrast should be privileged.

Finally, spectral and achromatic sensitivity may play an additional role in object detection. Arguably, colours are typically detectable only at high light levels and should not be used to generate contrast patterns alone (Land & Nilsson, 2012), also because the chromatic

spatial resolution is generally lower than the achromatic one in birds (Lind & Kelber, 2011, Potier et al., 2017a). However, our results indicated that black grouse have an intermediate near-UV-sensitive type of SWS1 cone, similarly to SWS1 cones in the pigeon *Columba livia* (Carvalho et al., 2007). Because the oil droplets in SWS1 photoreceptors are transparent (Hart, 2001), black grouse perceive short-wavelength light, offering the possibility to develop diverters that reflect UV or near-UV wavelengths invisible to humans. For instance, the use of UV lamps actively emitting short wavelengths (380-390 nm) on power poles has been shown to reduce night collisions of Sandhill Cranes *Grus canadensis* with power lines by 98% (Dwyer et al., 2019). Incorporating the use of natural surfaces reflecting short wavelengths in collision diverter design may be a promising avenue contributing to reducing bird collisions with man-made objects (Baasch et al., 2022). Therefore, although black grouse likely have limited visiual sensitivity in the short-wavelength range due to corneal filtering and the presence of filtering oil droplets in SWS2 cones, the use of diverters that reflect UV light would still be beneficial to reduce collisions. The reflectance properties of detection materials (Table S3) implemented in natural conditions were measured to gain a better understanding of the emission spectrum of diffuse and specular light rays (Figures S1-S8). By comparing a large diversity of diverters currently used to date in french Alps ski areas, we found that (1) most reflect visible wavelengths of light, but none of them reflect wavelengths shorter than 400 nm (UV range) and (2) some of them are using a red pattern reflecting wavelengths above 600 nm, reaching the limits of black grouse visual perception. Some diverters have already robust internal contrasts, suggesting that with little modification, such as increased size, improved contrast and short-wavelength reflective-material, improved diverters would allow better aerial cable detection by black grouse, a first step towards a significant reduction of risks of collisions.

Ethics

Ethical approval for the handling and restraint of birds was granted under the permit number APAFIS# 31775-31775-2021041311196892 v5. Permissions were granted from the owner of the birds used in the study.

Data accessibility

All data are available as electronic supplementary materials.

Authors' contributions

S.P.: conceptualization, data curation, investigation, methodology, visualisation, writing original draft, writing-review and editing. J.M.L.: data curation, methodology, writing original draft, writing-review and editing. C.B.: conceptualization, writing-review and editing. J.C.: conceptualization, writing-review and editing. V.D.S.: writing-review and editing. S.B.: conceptualization, writing-review and editing. C.A.: data curation, writing-review and editing. M.L.: conceptualization, data curation, investigation, methodology, visualisation, writing original draft, writing-review and editing. All authors gave final approval for publication and agreed to be held accountable for the work performed therein.

Conflict of interest declaration

The authors declare no competing interests.

Funding

This study was funded by the Vanoise National Parc as part of a European project entitled POIA BirdSki, with the assistance of the European Union and the National Agency for Cohesion of Territory under the Interregional Convention of the Alps massif, and in partnership with ASTERS-CEN74 and the Mountain Galliformes Observatory (OGM), with support from the FNADT – Alps Massif (National Fund for Territorial Planning and Development), and grants from the Swedish Research Council (2020-05107) and the Belgian F.R.S/FNRS (MISU F.6002.24) to MAL. JML is supported by a MISU grant from the FRS-FNRS (F.6002.22).

Acknowledgements

The authors would like to acknowledge Frank Grosemans for access to its birds, Pascal Barla for its expertise on spectral rays, the Fédération des Chasseurs de Savoie (FDC73) for its involvement in the collection of Black Grouse eyes. We finally thanks Catherine Desnos and Pascale Malchiodi for their help on building the opaque black cloth tent. The computations in this paper were run on the GIGA Cluster at ULiège.

References

Aidala, Z., Huynen, L., Brennan, P. L., Musser, J., Fidler, A., Chong, N., Machovsky Capuska, G. E., Anderson, M. G., Talaba, A., Lambert, D. & Hauber, M. E. 2012. Ultraviolet visual sensitivity in three avian lineages: paleognaths, parrots, and passerines. *Journal of Comparative Physiology A* **198**: 495-510.

Alerstam, T., Rosén, M., Bäckman, J., Ericson, P. G. P. & Hellgren, O. 2007. Flight Speeds among Bird Species: Allometric and Phylogenetic Effects. *PLOS Biology* **5**: e197.

Baasch, D. M., Caven, A. J., Jorgensen, J. G., Grosse, R., Rabbe, M., Varner, D. M. & LaGrange, T. 2022. Whooping Crane (*Grus americana*) use patterns in relation to an ecotope classification in the Central Platte River Valley, Nebraska, USA. *Avian Conservation and Ecology* **17**: 35.

Bech, N., Beltran, S., Boissier, J., Allienne, J., Resseguier, J. & Novoa, C. 2012. Bird mortality related to collisions with ski-lift cables: do we estimate just the tip of the iceberg? *Animal Biodiversity and Conservation* **35**: 95-98.

Bernardino, J., Bevanger, K., Barrientos, R., Dwyer, J. F., Marques, A. T., Martins, R. C., Shaw, J. M., Silva, J. P. & Moreira, F. 2018. Bird collisions with power lines: State of the art and priority areas for research. *Biological Conservation* **222**: 1-13.

Birch, D. & Jacobs, G. H. 1979. Spatial contrast sensitivity in albino and pigmented rats. *Vision Research* **19**: 933-7.

Bisti, S. & Maffei, L. 1974. Behavioural contrast sensitivity of the cat in various visual meridians. *Journal of Physiology* **241**: 201-10.

Blary, C. L. M., Duriez, O., Bonadonna, F., Mitkus, M., Caro, S. P., Besnard, A. & Potier, S. 2024. Low achromatic contrast sensitivity in birds: a common attribute shared by many phylogenetic orders. *Journal of Experimantal Biology* **227**: jeb246342.

Borges, R., Khan, I., Johnson, W. E., Gilbert, M. T. P., Zhang, G., Jarvis, E. D., O'Brien, S. J. & Antunes, A. 2015. Gene loss, adaptive evolution and the co-evolution of plumage coloration genes with opsins in birds. *BMC Genomics* **16**: 751.

Bowmaker, J. K. 1977. The visual pigments, oil droplets and spectral sensitivity of the pigeon. *Vision Research* **17**: 1129-1138.

Brainard, D. H. 1997. The Psychophysics Toolbox. *Spatial Vision* **10**: 433-6.

Brooke, M., Hanley, S. & Laughlin, S. 1999. The scaling of eye size with body mass in birds. *Proceedings of the Royal Society B: Biological Sciences* **266**: 405.

Bryant, D. M., Johnson, K., Tia, D., Tickle, T., Couger, M. B., Payzin-Dogru, D., Lee, T., Leigh, N., Kuo, T., Davis, F., Bateman, J., Bryant, S., Guzikowski, A., Tsai, S., Coyne, S., Ye, W., Freeman, R. J., Peshkin, L., Tabin, C., Regev, A., Haas, B. & Whited, J. 2017. A Tissue-Mapped Axolotl De Novo Transcriptome Enables Identification of Limb Regeneration Factors. *Cell reports* **18**: 762-776.

Buffet, N. & Dumont-Dayot, E. (2013) Bird collisions with overhead ski-cables: a reducible source of mortality. In: *The Impacts of Skiing and Related Winter Recreational Activities on Mountain Environments.* pp. 123-136. Eureka select.

Cantlay, J. C., Martin, G. R., McClelland, S. C., Potier, S., O'Brien, M. F., Fernández-Juricic, E., Bond, A. L. & Portugal, S. J. 2023. Binocular vision and foraging in ducks, geese and swans (Anatidae). *Proceedings of the Royal Society B: Biological Sciences* **290**: 20231213.

Carvalho, L. S., Cowing, J. A., Wilkie, S. E., Bowmaker, J. K. & Hunt, D. M. 2007. The molecular evolution of avian ultraviolet- and violet-sensitive visual pigments. *Molecular Biology and Evolution* **24**: 1843-52.

Carvalho, L. S., Knott, B., Berg, M. L., Bennett, A. T. D. & Hunt, D. M. 2011. Ultraviolet-sensitive vision in long-lived birds. *Proceedings of the Royal Society B: Biological Sciences* **278**: 107-114.

Caves, E. M., Fernández-Juricic, E. & Kelley, L. A. 2024. Ecological and morphological correlates of visual acuity in birds. *Journal of Experimental Biology* **227**: jeb246063.

Church, S. C., Bennett, A. T. D., Cuthill, I. C. & Partridge, J. C. 1998. Ultraviolet cues affect the foraging behaviour of blue tits. *Proceedings of the Royal Society B: Biological Sciences* **265**: 1509-1514.

Cooney, C. R., Varley, Z. K., Nouri, L. O., Moody, C. J. A., Jardine, M. D. & Thomas, G. H. 2019. Sexual selection predicts the rate and direction of colour divergence in a large avian radiation. *Nature Communications* **10**: 1773.

Corredor, V. H., Hauzman, E., Gonçalves, A. d. S. & Ventura, D. F. 2022. Genetic characterization of the visual pigments of the red-eared turtle (*Trachemys scripta elegans*) and computational predictions of the spectral sensitivity. *Journal of Photochemistry and Photobiology* **12**: 100141.

Crescitelli, F., Dvorak, C., Eder, D., Granda, A., Hamasaki, D., Holmberg, K., Hughes, A., Locket, N., McFarland, W., Meyer, D., Muntz, W., Munz, W., Olson, E. & Reyer, R. (1977) The avian eye and its adaptations. In: *The Visual System in Vertebrates*, (Crescitelli, F., ed.). pp. 549-611. Springer-Verlag, Berlin.

Cronin, T. W. & Bok, M. J. 2016. Photoreception and vision in the ultraviolet. *Journal of Experimental Biology* **219**: 2790-2801.

Crowell, H. L., Curlis, J. D., Weller, H. I. & Davis Rabosky, A. R. 2024. Ecological drivers of ultraviolet colour evolution in snakes. *Nature Communications* **15**: 5213.

Cuthill, I. C., Partridge, J. C., Bennett, A. T. D., Church, S. C., Hart, N. S. & Hunt, S. (2000) Ultraviolet Vision in Birds. In: *Advances in the Study of Behavior*, Vol. 29 (Slater, P. J. B., Rosenblatt, J. S., Snowdon, C. T. & Roper, T. J., eds.). pp. 159-214. Academic Press.

De Valois, R. L., Morgan, H. & Snodderly, D. M. 1974. Psychophysical studies of monkey Vision-III. Spatial luminance contrast sensitivity tests of macaque and human observers. *Vision Research* **14**: 75-81.

Dunning, J. 2007. *CRC Handbook of Avian Body Masses*. Boca Raton.

Dwyer, J., Pandey, A., McHale, L. & Harness, H. 2019. Near-ultraviolet light reduced Sandhill Crane collisions with a power line by 98%. *The Condor* **121**: 1-10.

Fernandez-juricic, E., Gall, M., Dolan, T., Tisdale, V. & Martin, G. 2008. The visual fields of two ground-foraging birds, House Finches and House Sparrows, allow for simultaneous foraging and anti-predator vigilance. *Ibis* **150**: 779-787.

Ferrer, M., Morandini, V., Baumbusch, R., Muriel, R., De Lucas, M. & Calabuig, C. 2020. Efficacy of different types of "bird flight diverter" in reducing bird mortality due to collision with transmission power lines. *Global Ecology and Conservation* **23**: e01130.

Finkbeiner, S. D. & Briscoe, A. D. 2021. True UV color vision in a female butterfly with two UV opsins. *Journal od Experimental Biology* **224**: jeb242802.

Frentiu, F. D. & Briscoe, A. D. 2008. A butterfly eye's view of birds. *BioEssays* **30**: 1151-1162.

Frick, H., Chow, F., Kuhn, M., Mahoney, M., Silge, J. & Wickham, H. (2022) Rsample: General Resampling Infrastructure. R package version 1.1.1. pp.

Ghim, M. M. & Hodos, W. 2006. Spatial contrast sensitivity of birds. *Journal of Comparative Physiology A* **192**: 523-34.

Goldsmith, T. H. 1990. Optimization, Constraint, and History in the Evolution of Eyes. *The Quarterly Review of Biology* **65**: 281-322.

Govardovskii, V., Fyhrquist, N., Reuter, T., Kuzmin, D. & Donner, K. 2000. In search of the visual pigment template. *Visual Neurosciences* **17**: 509-528.

Grabherr, M. G., Haas, B. J., Yassour, M., Levin, J. Z., Thompson, D. A., Amit, I., Adiconis, X., Fan, L., Raychowdhury, R., Zeng, Q., Chen, Z., Mauceli, E., Hacohen, N., Gnirke, A., Rhind, N., di Palma, F., Birren, B. W., Nusbaum, C., Lindblad-Toh, K., Friedman, N. & Regev, A. 2011. Full-length transcriptome assembly from RNA-Seq data without a reference genome. *Nature Biotechnology* **29**: 644.

Guillemain, M. & Fritz, H. 2002. Temporal variation in feeding tactics: exploring the role of competition and predators in wintering dabbling ducks. *Wildlife Biology* **8**: 81-90.

Günther, A., Dedek, K., Haverkamp, S., Irsen, S., Briggman, K. L. & Mouritsen, H. 2021. Double Cones and the Diverse Connectivity of Photoreceptors and Bipolar Cells in an Avian Retina. *The Journal of Neuroscience* **41**: 5015.

Hagen, J. F. D., Roberts, N. S. & Johnston, R. J. 2023. The evolutionary history and spectral tuning of vertebrate visual opsins. *Developmental Biology* **493**: 40-66.

Hall, M. I. & Ross, C. F. 2007. Eye shape and activity pattern in birds. *Journal of Zoology* **271**: 437-444.

Hart, N. S. 2001. The visual ecology of avian photoreceptors. *Progress in Retinal Eye Research* **20**: 675-703.

Hart, N. S. & Hunt, D. M. 2007. Avian visual pigments: characteristics, spectral tuning, and evolution. *The American Naturalist* **169**: S7-26.

Hauser, F. & Chang, B. 2017. Insights into visual pigment adaptation and diversity from model ecological and evolutionary systems. *Current opinion in genetics & development* **47**: 110-120.

Hauser, F. E., van Hazel, I. & Chang, B. S. W. 2014. Spectral tuning in vertebrate short wavelength-sensitive 1 (SWS1) visual pigments: Can wavelength sensitivity be inferred from sequence data? *Journal of Experimental Zoology* **322**: 529-539.

Hirsch, J. 1982. Falcon visual sensitivity to grating contrast. *Nature* **300**: 57-58.

Hunt, D. M., Carvalho, L. S., Cowing, J. A. & Davies, W. L. 2009. Evolution and spectral tuning of visual pigments in birds and mammals. *Philosophical Transactions of the Royal Society of London B Biolological Sciences* **364**: 2941-55.

Hunt, D. M., Carvalho, L. S., Cowing, J. A., Parry, J. W., Wilkie, S. E., Davies, W. L. & Bowmaker, J. K. 2007. Spectral tuning of shortwave-sensitive visual pigments in vertebrates. *Photochemistry and Photobiology* **83**: 303-10.

Hunt, D. M., Wilkie, S. E., Bowmaker, J. K. & Poopalasundaram, S. 2001. Vision in the ultraviolet. *Cellular and Molecular Life Sciences* **58**: 1583-98.

Jacobs, G. 1977. Visual capacities of the owl monkey (*Aotus trivirgatus*): II. Spatial contrast sensitivity. *Vision Research* **17**: 821-825.

Kelber, A. 2019. Bird colour vision - from cones to perception. *Current opinion in Behavioral Sciences* **30**: 34-40.

Keller, J., Strasburger, H., Cerutti, D. T. & Sabel, B. A. 2000. Assessing spatial vision - automated measurement of the contrast-sensitivity function in the hooded rat. *Journal of Neuroscience Methods* **97**: 103-10.

Kiltie, R. A. 2000. Scaling of visual acuity with body size in mammals and birds. *Functional Ecology* **14**: 226-234.

Knott, B., Berg, M. L., Morgan, E. R., Buchanan, K. L., Bowmaker, J. K. & Bennett, A. T. 2010. Avian retinal oil droplets: dietary manipulation of colour vision? *Proceedings of the Royal Society B: Biological Sciences* **277**: 953-62.

Kuhn, M. & Wickham, H. (2020) Tidymodels: a collection of packages for modeling and machine learning using tidyverse principles. . pp.

Land, M. F. & Nilsson, D. E. 2012. *Animal eyes*. Oxford, Oxford

Langmead, B. & Salzberg, S. L. 2012. Fast gapped-read alignment with Bowtie 2. *Nature Methods* **9**: 357-9.

Langston, A., Casagrande, V. A. & Fox, R. 1986. Spatial resolution of the galago. *Vision Research* **26**: 791-796.

Laughlin, S. B., de Ruyter van Steveninck, R. R. & Anderson, J. C. 1998. The metabolic cost of neural information. *Nature Neurosciences* **1**: 36-41.

Li, B. & Dewey, C. N. 2011. RSEM: accurate transcript quantification from RNA-Seq data with or without a reference genome. *BMC Bioinformatics* **12**: 323.

Liénard, M. A., Bernard, G. D., Allen, A., Lassance, J., Song, S., Childers, R., Yu, N., Ye, D., Stephenson, A., Valencia-Montoya, W., Salzman, S., Whitaker, M., Calonje M, Zhang, F. & Pierce, N. 2021. The evolution of red colour vision is linked to coordinated rhodopsin tuning in lycaenid butterflies. *PNAS* **118** e2008986118.

Liénard, M. A., Valencia-Montoya, W. A. & Pierce, N. E. 2022. Molecular advances to study the function, evolution and spectral tuning of arthropod visual opsins. *Philosophical Transactions of the Royal Society B: Biological Sciences* **377**: 20210279.

Lim, H. H. & Pike, T. W. 2016. Dietary carotenoid availability affects avian color discrimination. *Behavioral Ecology* **27**: 1579-1584.

Lind, O. & Kelber, A. 2011. The spatial tuning of achromatic and chromatic vision in budgerigars. *Journal of Vision* **11**: 2-2.

Lind, O., Mitkus, M., Olsson, P. & Kelber, A. 2014. Ultraviolet vision in birds: the importance of transparent eye media. *Proceedings of the Royal Society B: Biological Sciences* **281**: 20132209.

Lind, O., Sunesson, T., Mitkus, M. & Kelber, A. 2012. Luminance-dependence of spatial vision in budgerigars (*Melopsittacus undulatus*) and Bourke's parrots (*Neopsephotus bourkii*). *Journal of Comparative Physiology A* **198**: 69-77.

Lisney, T. J., Iwaniuk, A. N., Kolominsky, J., Bandet, M. V., Corfield, J. R. & Wylie, D. R. 2012. Interspecifc variation in eye shape and retinal topography in seven species of galliform bird (Aves: Galliformes: Phasianidae). *Journal of Comparative Physiology A* **198**: 717-31.

Marques, A. T., Batalha, H., Rodrigues, S., Costa, H., Pereira, M. J. R., Fonseca, C., Mascarenhas, M. & Bernardino, J. 2014. Understanding bird collisions at wind farms: An updated review on the causes and possible mitigation strategies. *Biological Conservation* **179**: 40-52.

Martin, G. 2011a. Understanding bird collisions with man-made objects: a sensory ecology approach. *Ibis* **153**: 239-254.

Martin, G. 2017. *The sensory ecology of birds*. Oxford University Press.

Martin, G. & Portugal, S. 2011. Differences in foraging ecology determine variation in visual fields in ibises and spoonbills (Threskiornithidae). *Ibis* **153**: 662-671.

Martin, G., Portugal, S. & Murn, C. 2012. Visual fields, foraging and collision vulnerability in Gyps vultures. *Ibis* **154**: 626-631.

Martin, G. R. 1984. The visual fields of the tawny owl, *Strix aluco* L. *Vision Research* **24**: 1739-1751.

Martin, G. R. 1986. Total panoramic vision in the mallard duck, *Anas platyrhynchos*. *Vision Research* **26**: 1303-5.

Martin, G. R. 1994. Visual fields in woodcocks *Scolopax rusticola* (Scolopacidae; Charadriiformes). *Journal of Comparative Physiology A* **174**: 787-793.

Martin, G. R. 2007. Visual fields and their functions in birds. *Journal of Ornithology* **148**: 547-562.

Martin, G. R. 2009. What is binocular vision for? A birds' eye view. *Journal of Vision* **9**: 14-14.

Martin, G. R. 2022. Vision-Based Design and Deployment Criteria for Power Line Bird Diverters. *Birds* **3**: 410-422.

Martin, G. R. & Banks, A. N. 2023. Marine birds: Vision-based wind turbine collision mitigation. *Global Ecology and Conservation* **42**: e02386.

Martin, M. 2011b. Cutadapt removes adapter sequences from high-throughput sequencing reads. *Embnet Journal* **17**: 3.

Massaro, M., Davis, L. S. & Darby, J. T. 2003. Carotenoid-derived ornaments reflect parental quality in male and female yellow-eyed penguins (*Megadyptes antipodes*). *Behavioral Ecology and Sociobiology* **55**: 169-175.

McCulloch, K. J., Yuan, F., Zhen, Y., Aardema, M. L., Smith, G., Llorente-Bousquets, J., Andolfatto, P. & Briscoe, A. D. 2017. Sexual Dimorphism and Retinal Mosaic Diversification following the Evolution of a Violet Receptor in Butterflies. *Molecular Biology and Evolution* **34**: 2271-2284.

Merigan, W. 1976. The contrast sensitivity of the squirrel monkey (*Saimiri sciureus*). *Vision Research* **16**: 375-379.

Moore, B. A., Pita, D., Tyrrell, L. P. & Fernández-Juricic, E. 2015. Vision in avian emberizid foragers: maximizing both binocular vision and fronto-lateral visual acuity. *Journal of Experimental Biology* **218**: 1347-1358.

Moran, D., Softley, R. & Warrant, E. J. 2015. The energetic cost of vision and the evolution of eyeless Mexican cavefish. *Science Advances* **1**: e1500363.

Nachtigall, P. G., Grazziotin, F. G. & Junqueira-de-Azevedo, I. L. M. 2021. MITGARD: an automated pipeline for mitochondrial genome assembly in eukaryotic species using RNA-seq data. *Briefings in Bioinformatics* **22**: bbaa429.

Niven, J. E. & Laughlin, S. B. 2008. Energy limitation as a selective pressure on the evolution of sensory systems. *Journal of Experimental Biology* **211**: 1792-804.

O'Rourke, C. T., Hall, M. I., Pitlik, T. & Fernández-Juricic, E. 2010. Hawk Eyes I: Diurnal Raptors Differ in Visual Fields and Degree of Eye Movement. *PLOS ONE* **5**: e12802.

Odeen, A. & Håstad, O. 2010. Pollinating birds differ in spectral sensitivity. *Journal of Comparative Physiology A* **196**: 91-6.

Olsson, P., Lind, O. & Kelber, A. 2017. Chromatic and achromatic vision: parameter choice and limitations for reliable model predictions. *Behavioral Ecology* **29**: 273-282.

Outomuro, D., Söderquist, L., Johansson, F., Ödeen, A. & Nordström, K. 2017. The price of looking sexy: visual ecology of a three-level predator–prey system. *Functional Ecology* **31**: 707-718.

Patel, J., Brown, C., Ytreberg, F. & Stenkamp, D. 2018. Predicting peak spectral sensitivities of vertebrate cone visual pigments using atomistic molecular simulations. *PLOS Computational Biology* **14**: e1005974.

Pérez i de Lanuza, G. & Font, E. 2014. Ultraviolet vision in lacertid lizards: evidence from retinal structure, eye transmittance, SWS1 visual pigment genes and behaviour. *Journal of Experimental Biology* **217**: 2899-909.

Portugal, S. J., Murn, C. P. & Martin, G. R. 2017. White-headed Vulture Trigonoceps occipitalis shows visual field characteristics of hunting raptors. *Ibis* **159**: 463-466.

Potier, S., Bonadonna, F., Kelber, A. & Duriez, O. 2016a. Visual acuity in an opportunistic raptor, the chimango caracara (*Milvago chimango*). *Physiology and Behavaviour* **157**: 125-8.

Potier, S., Bonadonna, F., Kelber, A., Martin, G. R., Isard, P.-F., Dulaurent, T. & Duriez, O. 2016b. Visual abilities in two raptors with different ecology. *Journal of Experimental Biology* **219**: 2639-2649.

Potier, S., Bonadonna, F., Martin, G. R., Isard, P.-F., Dulaurent, T., Mentek, M. & Duriez, O. 2017a. Visual configuration of two species of Falconidae with different foraging ecologies. *Ibis* **160**: 54-61.

Potier, S., Duriez, O., Cunningham, G. B., Bonhomme, V., O'Rourke, C., Fernández-Juricic, E. & Bonadonna, F. 2018. Visual field shape and foraging ecology in diurnal raptors. *Journal of Experimental Biology* **221**: jeb177295.

Potier, S., Lieuvin, M., Pfaff, M. & Kelber, A. 2020a. How fast can raptors see? *Journal of Experimental Biology* **223**: jeb209031.

Potier, S., Mitkus, M., Bonadonna, F., Duriez, O., Isard, P. F., Dulaurent, T., Mentek, M. & Kelber, A. 2017b. Eye Size, Fovea, and Foraging Ecology in Accipitriform Raptors. *Brain Behaviour and Evolution* **90**: 232-242.

Potier, S., Mitkus, M. & Kelber, A. 2020b. Visual adaptations of diurnal and nocturnal raptors. *Seminars in Cell & Developmental Biology* **106**: 116-126.

Potier, S., Roulin, A., Martin, G. R., Portugal, S. J., Bonhomme, V., Bouchet, T., de Romans, R., Meyrier, E. & Kelber, A. 2023. Binocular field configuration in owls: the role of foraging ecology. *Proceedings of the Royal Society B: Biological Sciences* **290**: 20230664.

Quast, C., Pruesse, E., Yilmaz, P., Gerken, J., Schweer, T., Yarza, P., Peplies, J. & Glöckner, F. O. 2013. The SILVA ribosomal RNA gene database project: improved data processing and web-based tools. *Nucleic Acids Research* **41**: D590-6.

Schmid, K. L. & Wildsoet, C. F. 1998. Assessment of visual acuity and contrast sensitivity in the chick using an optokinetic nystagmus paradigm. *Vision Research* **38**: 2629-2634.

Schneider, C. A., Rasband, W. S. & Eliceiri, K. W. 2012. NIH Image to ImageJ: 25 years of image analysis. *Nature Methods* **9**: 671-675.

Shi, Q. & Stell, W. K. 2013. Die Fledermaus: regarding optokinetic contrast sensitivity and light-adaptation, chicks are mice with wings. *PLoS One* **8**: e75375.

Shi, Y., Radlwimmer, F. & Yokoyama, S. 2001. Molecular genetics and the evolution of ultraviolet vision in vertebrates. *PNAS* **98**: 11731–11736.

Siitari, H., Viitala, J. & Hovi, M. 2002. Behavioural evidence for ultraviolet vision in a tetraonid species – foraging experiment with black grouse *Tetrao tetrix*. *Journal of Avian Biology* **33**: 199-202.

Simão, F. A., Waterhouse, R. M., Ioannidis, P., Kriventseva, E. V. & Zdobnov, E. M. 2015. BUSCO: assessing genome assembly and annotation completeness with single-copy orthologs. *Bioinformatics* **31**: 3210-2.

Song, L. & Florea, L. 2015. Rcorrector: efficient and accurate error correction for Illumina RNA-seq reads. *GigaScience* **4**: 48.

Spiegel, O., Getz, W. M. & Nathan, R. 2013. Factors Influencing Foraging Search Efficiency: Why Do Scarce Lappet-Faced Vultures Outperform Ubiquitous White-Backed Vultures? *The American Naturalist* **181**: E102-E115.

Toomey, M. B., Collins, A. M., Frederiksen, R., Cornwall, M. C., Timlin, J. A. & Corbo, J. C. 2015. A complex carotenoid palette tunes avian colour vision. *Journal of The Royal Society Interface* **12**: 20150563.

van Hazel, I., Sabouhanian, A., Day, L., Endler, K. & Chang, B. 2013. Functional characterization of spectral tuning mechanisms in the Great Bowerbird short-wavelength sensitive visual pigment (SWS1), and the origins of UV/violet vision in passerines and parrots. *BMC Evol Biol* **13**: 250.

Wagner, H., Pappe, I. & Nalbach, H. O. 2022. Optocollic responses in adult barn owls (*Tyto furcata*). *Journal of Comparative Physiology A* **208**: 239-251.

Witter, M. S. & Cuthill, I. C. 1993. The ecological costs of avian fat storage. *Philosophical Transactions of the Royal Society of London B Biological Sciences* **340**: 73-92.

Wu, Y., Hadly, E. A., Teng, W., Hao, Y., Liang, W., Liu, Y. & Wang, H. 2016. Retinal transcriptome sequencing sheds light on the adaptation to nocturnal and diurnal lifestyles in raptors. *Scientific Reports* **6**: 33578.

Yokoyama, S., Tada, T., Liu, Y., Faggionato, D. & Altun, A. 2016. A simple method for studying the molecular mechanisms of ultraviolet and violet reception in vertebrates. *BMC Evolutionary Biology* **16**: 64.

Supplementary materials

Supplementary methods

Firefly and ski cable properties

Reflectance measurements were carried out using a high-performance spectrophotometer, Cary 5000 UV-Vis-NIR spectrophotometer (Agilent) capturing wavelengths from 300 to 800 nm (PM detector) with a data interval of 1 nm. A reference blank (spectralon) was used for baseline before each measurement. A wide range of detection devices already installed in ski resort stations were sampled (Table S4). The majority of materials were opaque, therefore not transmitting light rays and preventing measures of light transmission. Two types of reflection were measured, i) diffuse reflection, when the light is reflected in many directions, and ii) diffuse + specular reflection, when the incident ray gives rise to a single reflected ray. Specular reflection corresponds to direct reflection and is generally perceptible at a greater distance than diffuse reflection. Most visual situations combine both diffuse and specular reflection, which we measured separately.

Supplementary results

Reflectance spectra of cable detection devices

Reflection characteristics for different materials used to build detection devices are presented in Figures S1 to S8, with ultraviolet light below 400 nm and long-wavelength light above 750 nm, coloured in black. For most materials, except the shiny stainless-steel plate (Fig. S7), the specular ray is identical to the diffuse ray. The diversity of existing devices shows a diversity of spectral reflection of visible light, whereas few materials reflect in the ultraviolet part of the light spectrum. In some instances, measured relative reflectance is higher than 100% owing to fluorescent components of certain material designs that store light to release it afterwards.

Reflection spectra also allow us to identify devices that exhibit highest achromatic contrasts (Flags and Firefly for instance, Figs. S3-S4). Hence, greater differences in reflectance spectra of spatially closed material will convey a greater internal achromatic contrast.

Supplementary Datasets:

Dataset 1: Opsin sequences

Dataset 2: Opsin absorbance values

Supplementary Tables

Table S1: Steps used for the contrast sensitivity estimation and their associated contrasts (of the vertical sinusoidal achromatic gratings) and the average luminance of the screens.

Step	Michelson Contrast	Inverse Michelson Contrast	Average luminance
127	1.00	1.00	130.26
120	1.00	1.00	124.79
110	0.99	1.01	116.42
100	0.97	1.03	107.09
90	0.94	1.07	99.86
80	0.90	1.11	93.51
70	0.85	1.18	87.80
60	0.78	1.29	82.73
50	0.69	1.45	77.88
45	0.64	1.57	75.36
40	0.58	1.71	73.18
35	0.52	1.92	71.24
30	0.46	2.17	69.79
29	0.45	2.24	69.33
28	0.43	2.31	68.97
27	0.42	2.39	68.53
26	0.40	2.47	68.28
25	0.39	2.55	67.95
24	0.38	2.65	67.89
23	0.37	2.74	67.31
22	0.35	2.88	67.21
21	0.33	2.99	67.06
20	0.32	3.13	66.67
19	0.30	3.29	66.57
18	0.29	3.45	66.34
17	0.27	3.64	66.09
16	0.26	3.84	65.88
15	0.24	4.10	65.57
14	0.23	4.39	65.33
13	0.21	4.71	65.21
12	0.20	5.07	64.98
11	0.18	5.50	64.71

10	0.17	6.04	64.62
9	0.15	6.62	64.49
8	0.13	7.50	64.13
7	0.12	8.51	63.96
6	0.10	9.62	63.78
5	0.09	11.46	63.57
4	0.07	13.89	63.50
3.5	0.06	16.12	64.05
3	0.05	18.32	63.54
2.5	0.05	21.70	64.04
2	0.04	26.73	63.35
1.5	0.03	35.39	63.89
1	0.02	51.29	63.23
0.5	0.01	82.54	63.76

Table S2: Oligonucleotide primers

ORF primers	Sequence (5' - 3')	ORF size (bp)
s,forward; as, reverse		
Lte-SWS1-ORF-HindIII-s	*ggtgcc*AAGCTT**GCCACC**ATG**G**CCTCGGACGACGACTTCTACCT	1,044
Lte-SWS1-ORF-BsiWI-as	*cggccg*CGTACGAGTGGGGCTGACCTGGCTGG	
Lte-SWS2-ORF-AflII-s	*ggtgcc*CTTAAG**GCCACC**ATG**G**ACCCCCCTCGCCCCC	1,071
Lte-SWS2-ORF-BsiWI-as	*cggccg*CGTACGGGCGGGCGAGACGGAGG	
Lte-Rh2-ORF-HindIII-s	*ggtgcc*AAGCTT**GCCACC**ATG**G**GACAGAAGGTATCAATTTTTA	1,068
Lte-Rh2-ORF-BsiWI-as	*cggccg*CGTACGTGCAGGTGATACTTGGCTGGAGG	
Lte-LW-ORF-HindIII-s	*ggtgcc*AAGCTT**GCCACC**ATG**G**AGGAGTGGGAGGCGGCG	1,089
Lte-LW-ORF-BsiWI-as	*cggccg*CGTACGGGCGGGCGAGACGGAGGA	
pcDNA5-FLAG_T2A-mruby2 construct verification primers		
pcDNA5-s	GCTGTTTTGACCTCCATAGAAGA	-
pcDNA5-as	TAGAAGGCACAGTCGAGG	-
pLenti-s	ACCGCATGTTAGCAGACTT	-
mRuby-as	CGGCGGCTTAAACCTTATCGTCG	-

bases with underlined capital letters: restriction sites;bases in italics: extra bases; bases in bold: Kozak

Table S3: Presentation of sampled devices.

Type	**Photography**
Spirale avifaune Installation on the multipair of chairlifts product abandoned to date Size: 30 cm x 4 cm	
Transparent float (test version) Installation on safety rope of ski lifts Size: 7.5 cm X 4.5	
Opaque float (OGM Flotteur) Installation on safety rope of ski lifts Size: 7.5 cm X 4.5	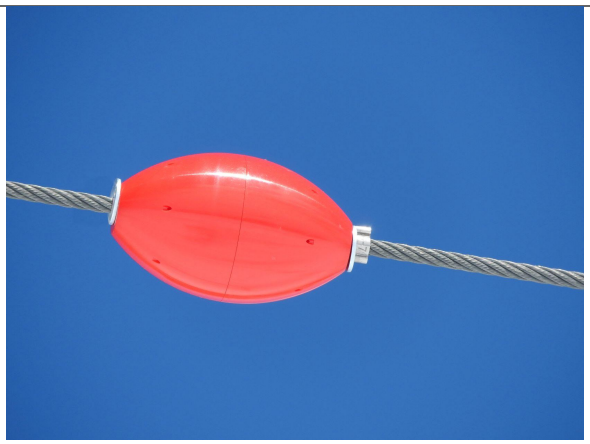

Fluorescent tube (material used to equip the guy cables) Size: 15 cm x 3.5 cm	
Shiny stainless-steel plate In test To equip aerial cables for transporting explosives Size: 8 x 8 cm	
Matte stainless-steel plate Size: 8 x 8 cm	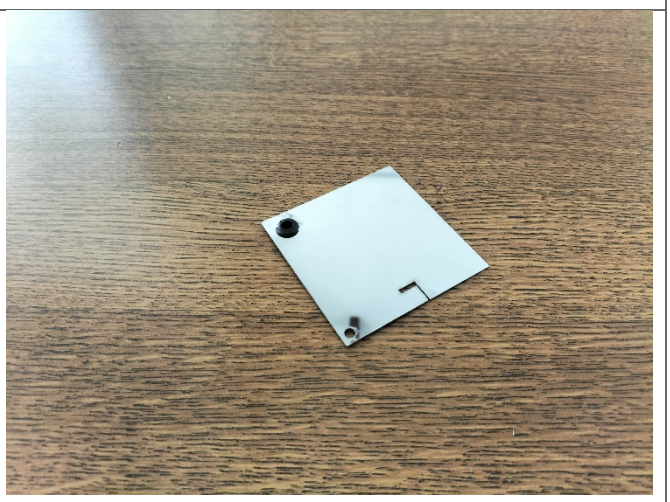

White Birdmark (stores light that is reflected at night) Installation on the multipair of chairlifts, gondola and on safety rope of ski lifts Installation recommendation: Alternation White Birdmark and Orange Birdmark Size: Racket diameter = 13.5 cm	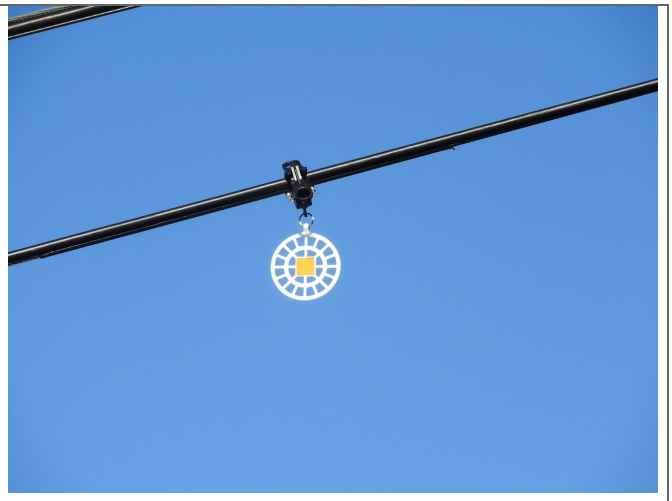
Orange Birdmark Installation on the multipair of chairlifts, gondola and on safety rope of ski lifts Installation recommendation: Alternation White Birdmark and Orange Birdmark Size: Racket diameter = 13.5 cm	
Crocfast (test) Size: Racket diameter = 13.5 cm	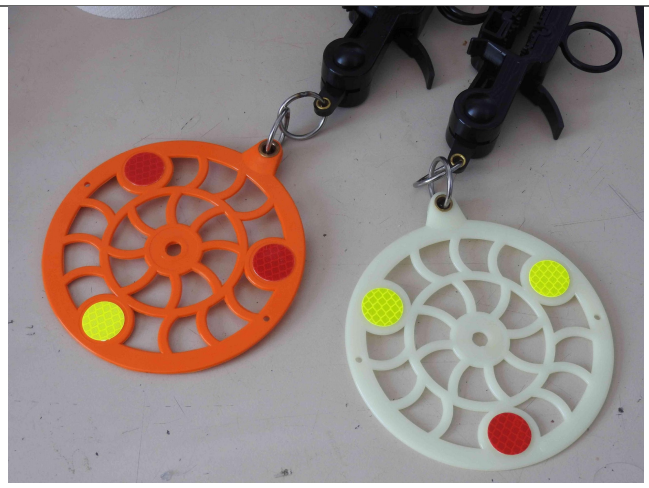

Firefly Ultra Alps Installation on the multipair of chairlifts and gondola Size: 15 cm x 9 cm	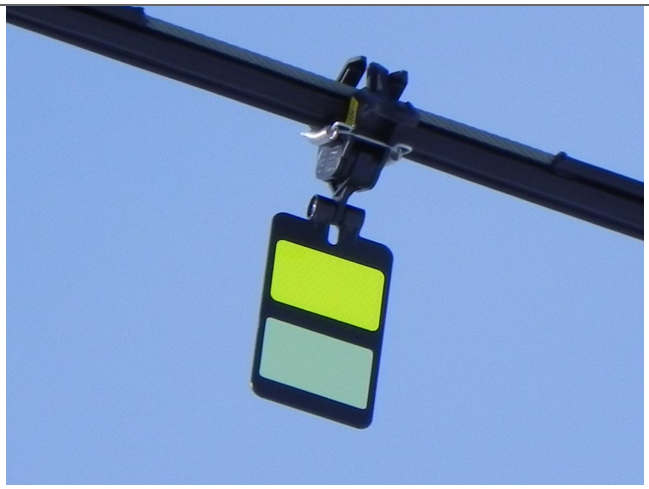
Firefly (equipment for power lines) Size: 15 cm x10.5 cm	
Flag (To equip aerial cables for transporting explosives) Size: 16x16 cm	

1

Supplementary Figures

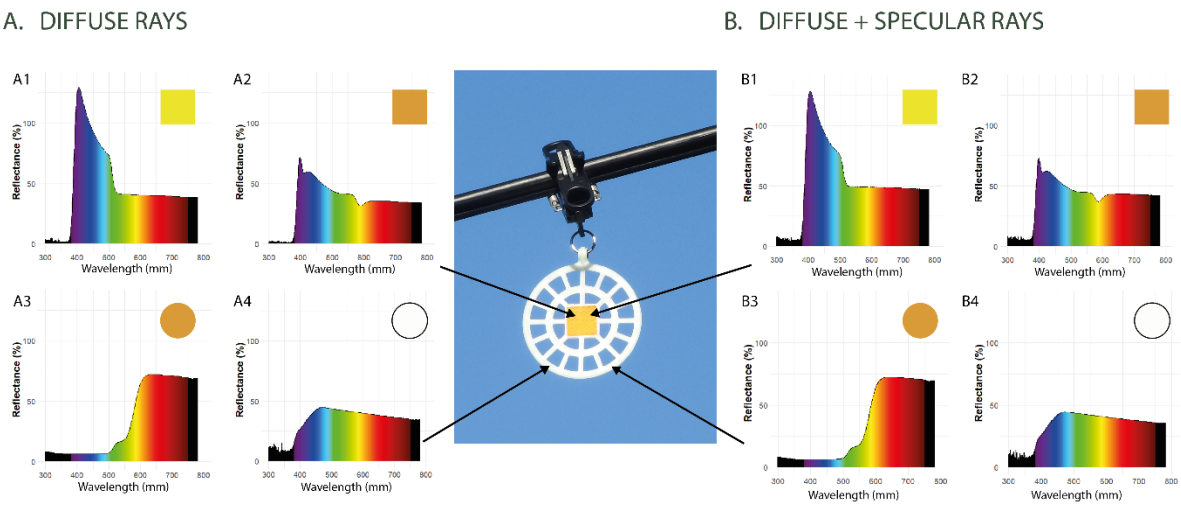

Figure S1. Reflection characteristics of diffuse and specular reflection of Birdmarks. A1 and B1 correspond to the yellow retroreflector, A2 and B2 correspond to the orange retroreflector, A3 and B3 correspond to an orange paddle, and A4 and B4 correspond to a white paddle.

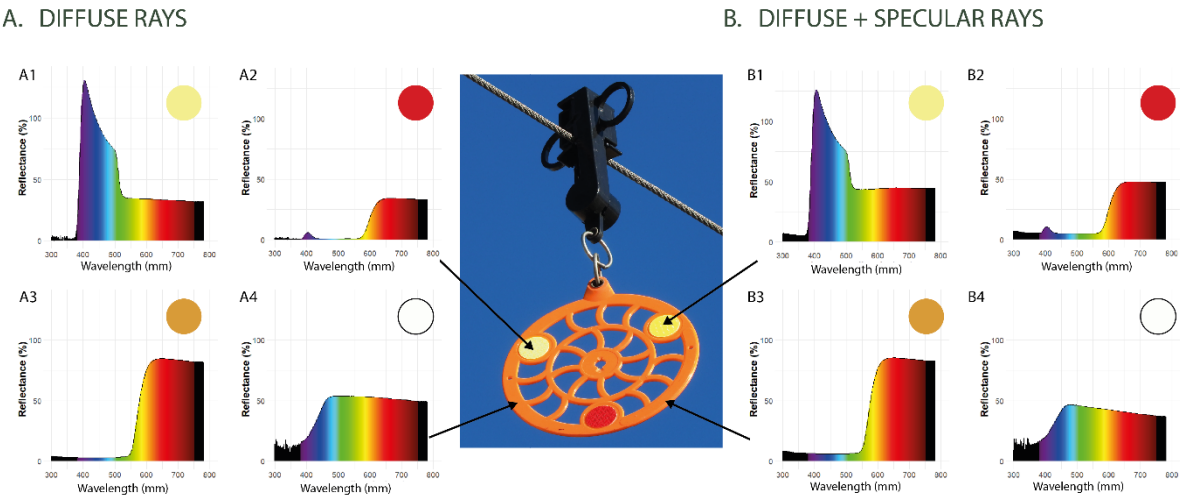

Figure S2. Reflection characteristics of diffuse and specular reflection of Crocfast. A1 and B1 correspond to the yellow retroreflector, A2 and B2 correspond to the red retroreflector, A3 and B3 correspond to an orange paddle, and A4 and B4 correspond to a white paddle.

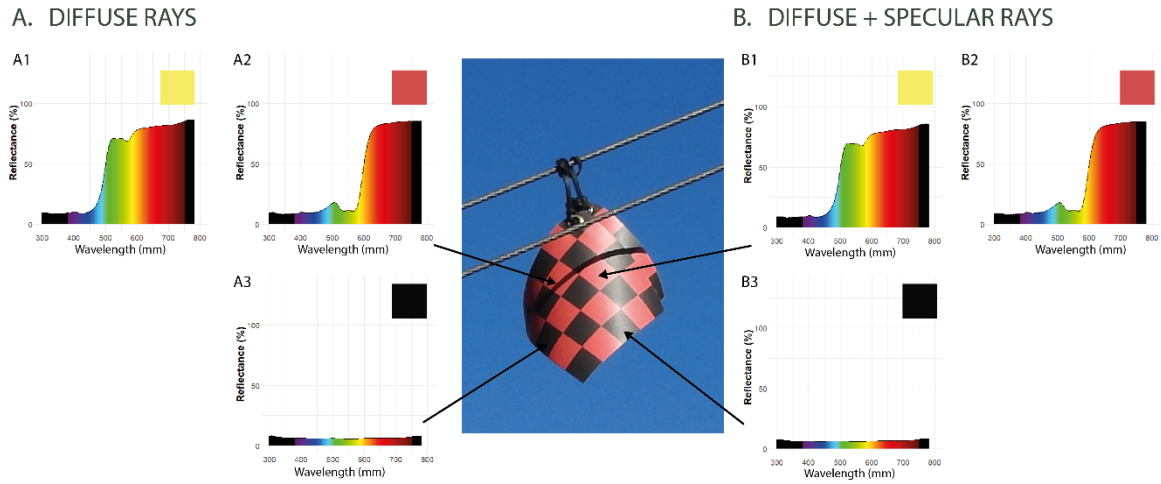

Figure S3. Reflection characteristics of diffuse and specular reflection of Flags. A1 and B1 correspond to a yellow square, A2 and B2 correspond to a red square, and A3 and B3 correspond to a black square.

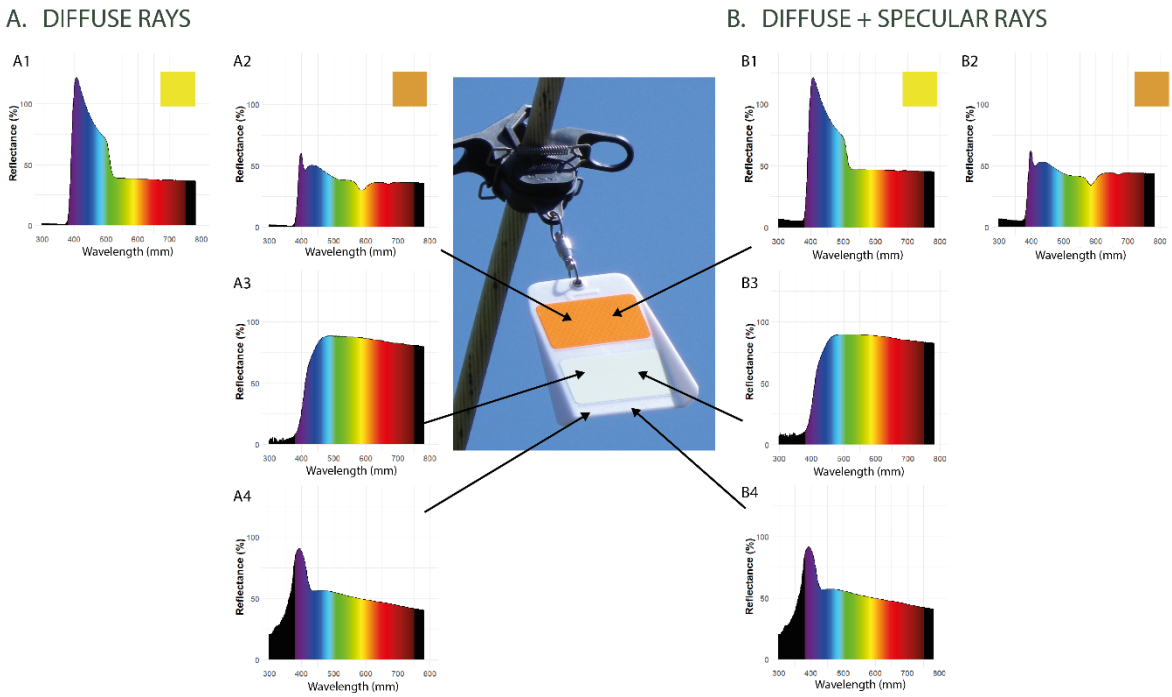

Figure S4. Reflection characteristics of diffuse and specular reflection of white Fireflies. A1 and B1 correspond to the yellow retroreflector, A2 and B2 correspond to the orange retroreflector, A3 and B3 correspond to the phosphorescent retroreflector, and A4 and B4 correspond to a white beacon.

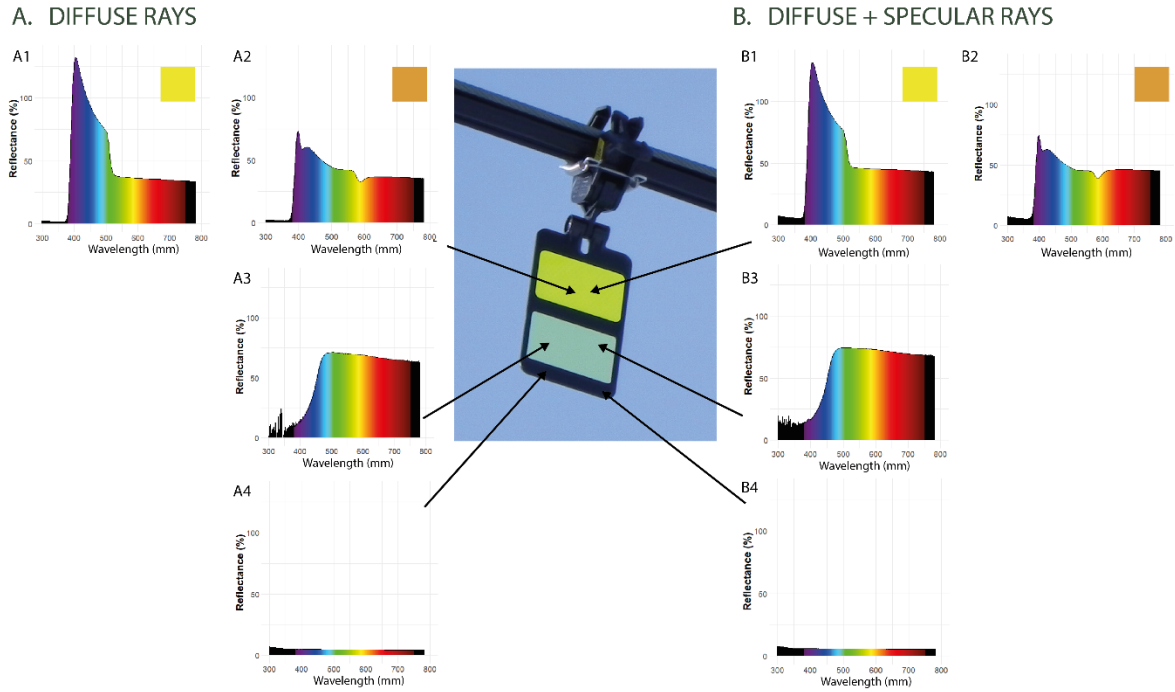

Figure S5. Reflection characteristics of diffuse and specular reflection of black Fireflies. A1 and B1 correspond to the yellow retroreflector, A2 and B2 correspond to the orange retroreflector, A3 and B3 correspond to the phosphorescent retroreflector, and A4 and B4 correspond to a black beacon.

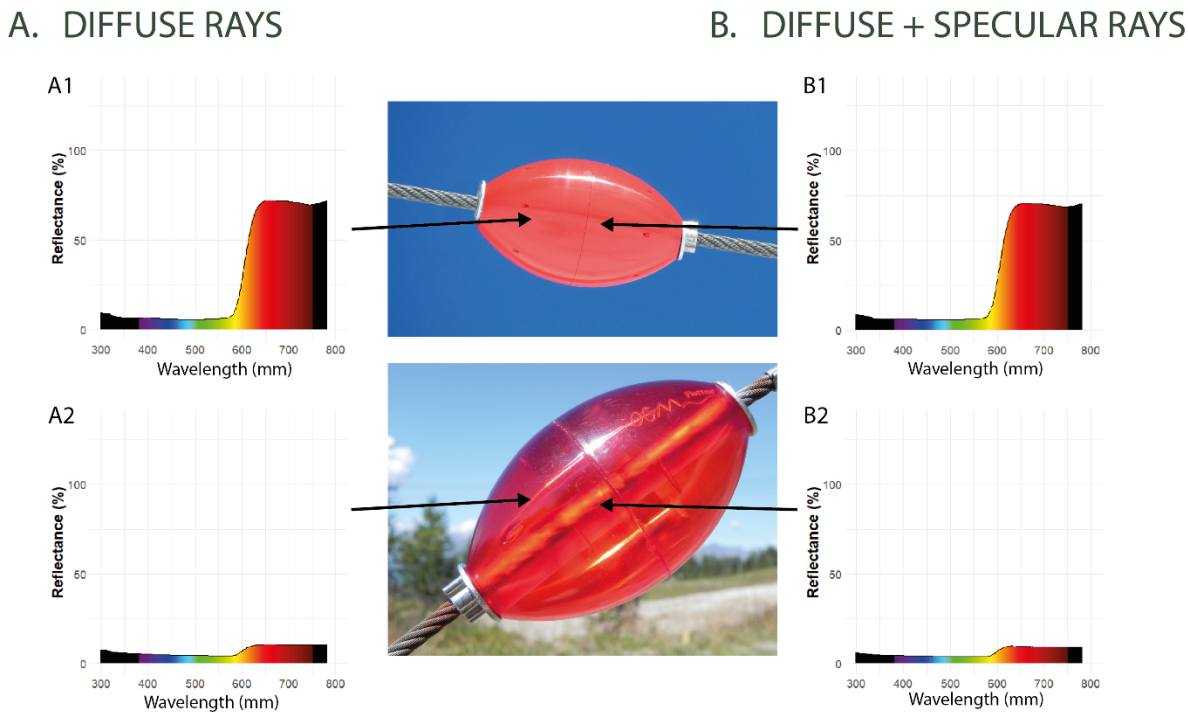

Figure S6. Reflection characteristics of diffuse and specular reflection of Floats. A1 and B1 correspond to a transparent float, and A2 and B2 correspond to an opaque float.

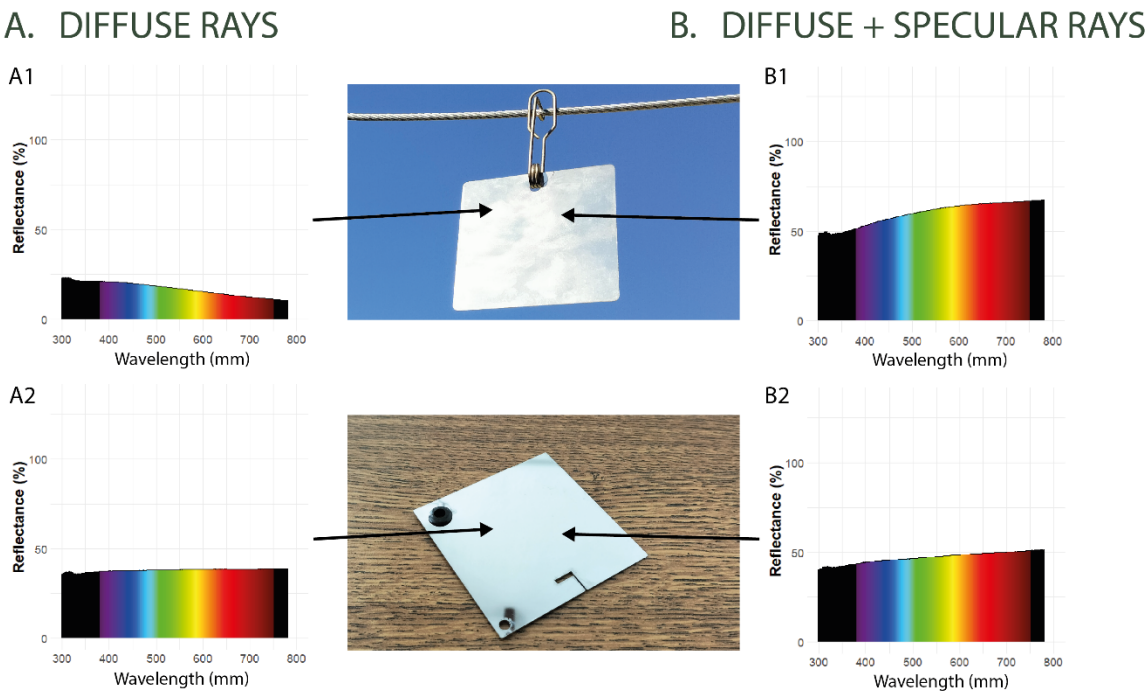

Figure S7. Reflection characteristics of diffuse and specular reflection of stainless-steel plates. A1 and B1 correspond to a shiny plate, and A2 and B2 correspond to a matte plate.

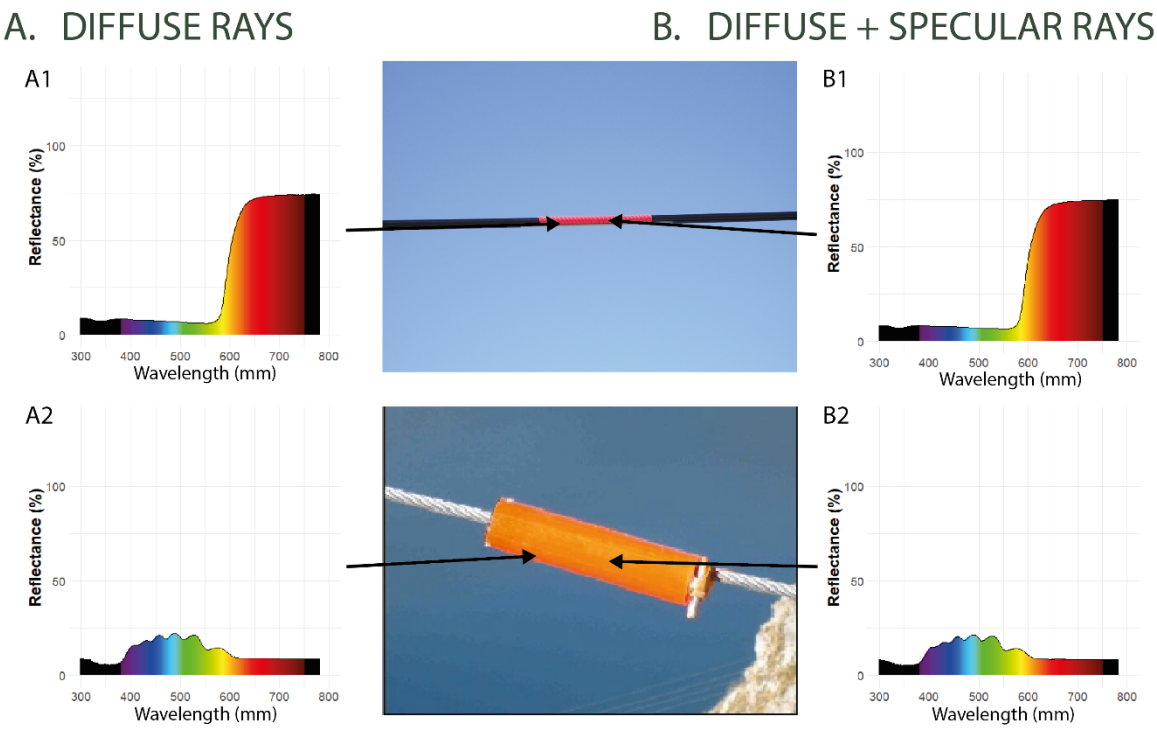

Figure S8. Reflection characteristics of diffuse and specular reflection of spirals and fluorescent tubes. A1 and B1 correspond to a red spiral, and A2 and B2 correspond to a fluorescent tube.

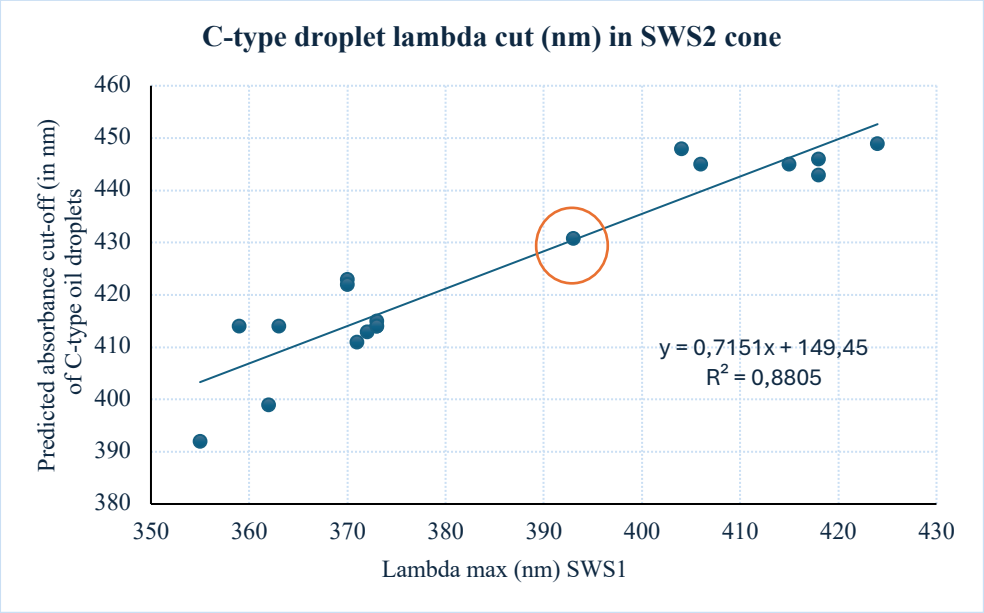

Figure S9. C-type droplet lambda cut-off. The orange circle is the predicted value for *L. tetrix* based on values from Hart (2001).

Hart, N. S. 2001. The visual ecology of avian photoreceptors. *Prog Retin Eye Res* **20**: 675-703.